or **9** was accurately weighed (ca. 0.05 g) into a series of 5-mm NMR tubes. Toluene-d_8 (ca. 0.25 mL) was added. The samples were heated to appropriate temperatures within the NMR spectrometer, and a series of ^{1}H NMR spectra were collected every 5–6 min for approximately 2–3 h. The integrations of the *tert*-butyl proton resonances were used to determine the relative quantity of each species. Rate constants were calculated from plots of ln [Al-Et] versus time and k_{obs} versus [O=CPh$_2$], while ΔH^* and ΔS^* were calculated from the appropriate Eyring plots.

Acknowledgment. We thank the Aluminum Research Board and the Milton Foundation for financial support. We are indebted to one of the reviewers for comments; this paper is more readable because of them.

OM910784C

Scope and Diastereoselectivity of Intramolecular [4 + 2] Diels–Alder Cycloadditions within the Coordination Sphere of $[(\eta^5\text{-}C_5H_5)Ru(DMPP)_{3-n}(dienophile)_n]PF_6$

Hong-Li Ji,[1a] John H. Nelson,*[1a] Andre De Cian,[1b] Jean Fischer,[1b] Ljiljana Solujić,[1c] and Emil B. Milosavljević[1c]

Department of Chemistry, University of Nevada, Reno, Nevada 89557, Laboratoire de Cristallochimie et de Chimie Structurale (URA424-CNRS), Université Louis Pasteur, 67070 Strasbourg Cedex, France, and Faculty of Sciences, University of Belgrade, 11001 Belgrade, Yugoslavia

Received October 31, 1991

The complex $[(\eta^5\text{-}C_5H_5)Ru(DMPP)_2(CH_3CN)]PF_6$ (**1**; DMPP = 1-phenyl-3,4-dimethylphosphole) reacts with the dieneophiles $Ph_2PCH{=}CH_2$ (DPVP), $PhP(CH{=}CH_2)_2$ (DVPP), $PhP(CH_2CH{=}CH_2)_2$ (DAPP), $PhS(O)CH{=}CH_2$, $PhSCH{=}CH_2$, and 2-vinylpyridine to produce one (**10**, **12**), two (**4**, **11**), or three (**5**, **9**) diastereomers of (η^5-cyclopentadienyl)(1-phenyl-3,4-dimethylphosphole)[*syn-exo*-2-(diphenylphosphino)-5,6-dimethyl-7-phenyl-7-phosphabicyclo[2.2.1]hept-5-ene]ruthenium(II) hexafluorophosphate (**4a**,**b**), (η^5-cyclopentadienyl)(1-phenyl-3,4-dimethylphosphole)[*syn-exo*-2-(phenylvinylphosphino)-5,6-dimethyl-7-phenyl-7-phosphabicyclo[2.2.1]hept-5-ene]ruthenium(II) hexafluorophosphate (**5a**,**b**), (η^5-cyclopentadienyl){*syn-exo-meso*-phenylbis[5,6-dimethyl-7-phenyl-7-phosphabicyclo[2.2.1]hept-5-en-2-yl]phosphine}ruthenium(II) hexafluorophosphate (**5c**), (η^5-cyclopentadienyl)(1-phenyl-3,4-dimethylphosphole)[*syn-exo*-2-((allylphenylphosphino)methyl)-5,6-dimethyl-7-phenyl-7-phosphabicyclo[2.2.1]-hept-5-ene]ruthenium(II) hexafluorophosphate (**9a**,**b**), (η^5-cyclopentadienyl){*syn*-exo-*dl*-phenylbis[(5,6-dimethyl-7-phenyl-7-phosphabicyclo[2.2.1]hept-5-ene-2-yl]phosphine}ruthenium(II) hexafluorophosphate (**9c**), (η^5-cyclopentadienyl)(1-phenyl-3,4-dimethylphosphole)[*syn-exo*-2-(phenylsulfinyl)-5,6-dimethyl-7-phenyl-7-phosphabicyclo[2.2.1]hept-5-ene]ruthenium(II) hexafluorophosphate (**10**), (η^5-cyclopentadienyl)(1-phenyl-3,4-dimethylphosphole)[*syn-exo*-2-(phenylthio)-5,6-dimethyl-7-phenyl-7-phosphabicyclo[2.2.1]hept-5-ene]ruthenium(II) hexafluorophosphate (**11**), (η^5-cyclopentadienyl)[*syn-exo*-2-(2-pyridyl)-5,6-dimethyl-7-phenyl-7-phosphabicyclo[2.2.1]hept-5-ene]ruthenium(II) hexafluorophosphate (**12**), respectively, by intramolecular [4 + 2] Diels–Alder cycloadditions in high yields. Similar Diels–Alder cycloadditions occur with $[(\eta^5\text{-}C_5H_5)Ru(DPVP)_2(CH_3CN)]PF_6$ (**2**) and $[(\eta^5\text{-}C_5H_5)Ru(DVPP)_2(CH_3CN)]PF_6$ (**3**) and DMPP to form **6a**,**b** and **7a**,**b**, respectively. Reactions of **1** with the potential dienophilic ligands L = $Me_2NC(O)CH{=}CH_2$, $PhS(O)_2CH{=}CH_2$, $P(OCH_2CH{=}CH_2)_3$, $P(C{\equiv}CPh)_3$, $H_2NCH_2CH{=}CH_2$, $N{\equiv}C{-}CH{=}CH_2$, $N(CH_2C(CH_3){=}CH_2)_3$, and $C_2H_5OCH{=}CH_2$ produced the $[(\eta^5\text{-}C_5H_5)Ru(DMPP)_2L)]PF_6$ complexes **14**–**21**, which could not be induced to undergo subsequent [4 + 2] Diels–Alder cycloadditions. New complexes were characterized by elemental analyses, physical properties, cyclic voltammetry, infrared spectroscopy, and ^{1}H, ^{13}C{^{1}H}, ^{31}P{^{1}H}, and in some cases by ^{1}H{^{31}P} nuclear magnetic resonance spectroscopy. Complex **11** is stereochemically nonrigid with sulfur inversion occurring rapidly at room temperature; $\Delta G^* = 59.8$ kJ mol^{-1}. The structures of **4b**, **5c**, and **11** were confirmed by X-ray crystallography. They crystallize in the $P2_1/c$, $P2_1/m$, and $C2/c$ space groups, respectively, in unit cells of the following dimensions: **4b**, $a = 20.965$ (9) Å, $b = 11.125$ (4) Å, $c = 21.678$ (9) Å, $\beta = 118.26$ (2)°, ρ(calcd) = 1.438 g cm^{-3}, $Z = 4$; **5c**, $a = 11.137$ (3) Å, $b = 19.124$ (5) Å, $c = 8.686$ (3) Å, $\beta = 102.93$ (2)°, ρ(calcd) = 1.564 g cm^{-3}, $Z = 2$; **11**, $a = 11.392$ (2) Å, $b = 19.018$ (5) Å, $c = 35.610$ (8) Å, $\beta = 96.40$ (2)°, ρ(calcd) = 1.429 g cm^{-3}, $Z = 8$. Refinements converged to $R(F) = 0.051$, 0.042, and 0.048 for 4842, 1975, and 3178 independent observed ($I \geq 3\sigma(I)$) reflections, respectively.

Introduction

We have recently shown that a series of new conformationally rigid chelating ligands could be readily obtained by metal-promoted intramolecular [4 + 2] Diels–Alder cycloadditions of 1-phenyl-3,4-dimethylphosphole (DMPP) and various dienophiles.[2-8]

The DMPP ligand shows distinct chemistry from other phosphorus ligands.[9-13] Its facile reaction with good

(1) (a) University of Nevada. (b) Université Louis Pasteur. (c) University of Belgrade.

(2) Solujić, L.; Milosavljević, E. B.; Nelson, J. H.; Alcock, N. W.; Fischer, J. *Inorg. Chem.* **1989**, *28*, 3453.
(3) Holt, M. S.; Nelson, J. H.; Savignac, P.; Alcock, N. W. *J. Am. Chem. Soc.* **1985**, *107*, 6939.
(4) Rahn, J. A.; Holt, M. S.; Gray, G. A.; Alcock, N. W.; Nelson, J. H. *Inorg. Chem.* **1989**, *28*, 217.
(5) Rahn, J. A.; Holt, M. S.; Nelson, J. H. *Polyhedron* **1989**, *8*, 897.

0276-7333/92/2311-1840$03.00/0

Chart I

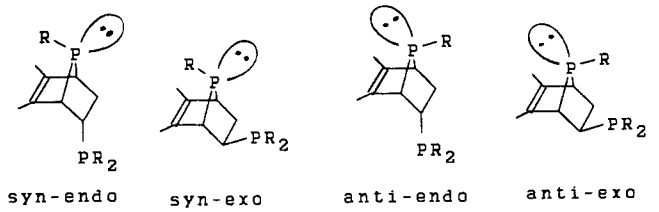

dienophiles, in both the presence and absence of metals, was first reported by Mathey and co-workers (reactions 1–3).[14] DMPP reacts with *N*-phenylmaleimide (reaction

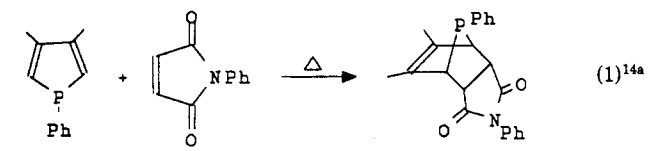
(1)[14a]

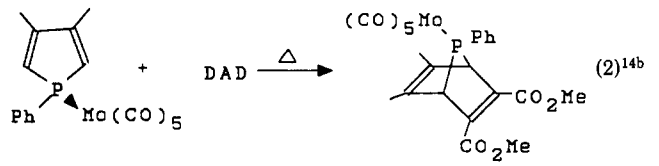
(2)[14b]

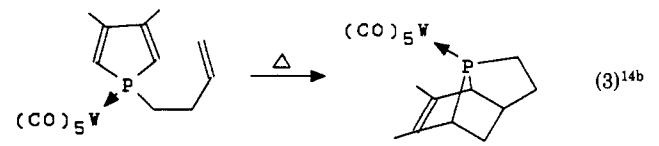
(3)[14b]

1) to give exclusively the anti-endo stereoisomer. $(DMPP)Mo(CO)_5$ reacts with dimethyl acetylenedicarboxylate (DAD; reaction 2) to give the anti product wherein the bimolecular cycloaddition of DAD takes place on the less hindered side of the coordinated phosphole. Reaction 3 depicts an intramolecular Diels–Alder cycloaddition leading to a tricyclic phosphine.

We recently discovered[2-8] that intramolecular cycloaddition of DMPP with a coordinated dienophile readily occurs within the coordination sphere of a transition metal, affording a series of novel, conformationally rigid, asymmetric bidentate ligands, 2-phosphino-7-phosphabicyclo-[2.2.1]hept-5-enes. Of the four possible products (Chart I) in these reactions the intramolecular cycloaddition gives exclusively the syn-exo diastereomer as illustrated in reactions 4 and 5. Similar reactions were also found to occur[2] within the coordination sphere of nickel(II) (reaction 6), where a new triphosphine ligand was formed. Analo-

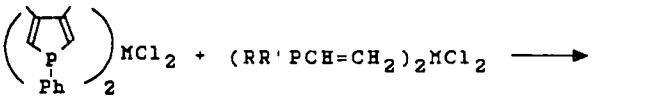

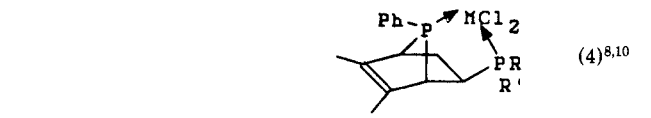
(4)[8,10]

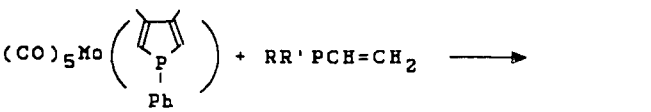

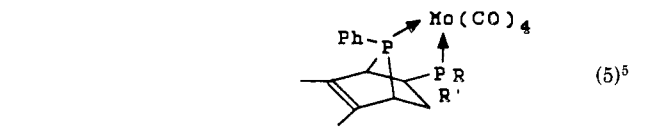
(5)[5]

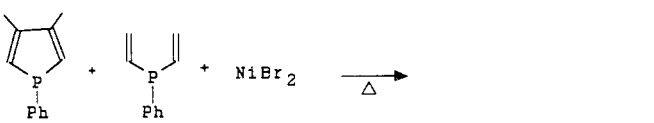

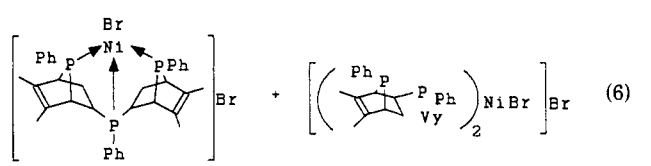
(6)

gous reactions between *ttt*-$(DMPP)_2Ru(CO)_2Cl_2$ and non-phosphine dienophiles produced[6,7] new types of hemilabile[15] bidentate ligands (reactions 7 and 8).

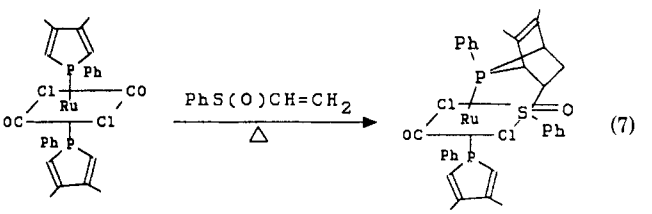
(7)

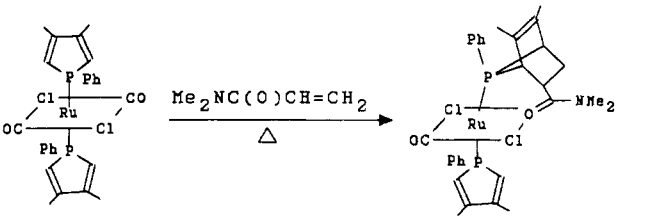
(8)

The diastereoselectivity in reactions 4–8 is often rather high, but except for reactions 7 and 8, the nature of the dieneophile that will participate in these reactions has been limited to vinylphosphines. In an effort to expand the scope of these reactions, and to gain greater insight into the factors controlling the diastereoselectivity, we have studied the reactions of $[(\eta^5\text{-}C_5H_5)Ru(DMPP)_2(CH_3CN)]PF_6$ with a variety of dienophiles and report the results herein. Our overall goal in this research is to develop general processes for the syntheses of conformationally rigid bidentate and tridentate ligands with defined stereochemistry that possess a variety of different donor atoms.

Experimental Section

A. Reagents and Physical Measurements. Hydrated ruthenium trichloride (43.02% Ru, Matthey Bishop), Ph_3P (M and T chemicals), C_5H_5Tl, 1,3-cyclohexadiene, NH_4PF_6, H_2NCH_2C-

(6) Green, R. L.; Nelson, J. H.; Fischer, J. *Organometallics* **1987**, *6*, 2256.

(7) Vac, R.; Nelson, J. H.; Milosavljević, E. B.; Solujić, L.; Fischer, J. *Inorg. Chem.* **1989**, *28*, 4132.

(8) Affandi, S.; Nelson, J. H.; Fischer, J. *Inorg. Chem.* **1989**, *28*, 4536.

(9) Mathey, F. *Top. Phosphorus Chem.* **1980**, *10*, 1.

(10) Mathey, F.; Fischer, J.; Nelson, J. H. *Struct. Bonding (Berlin)* **1983**, *55*, 153.

(11) Nelson, J. H.; Mathey, F. In *Phosphorus-31 NMR Spectroscopy in Stereochemical Analysis*; Verkade, J. G., Quin, L. D., Eds.; VCH: Deerfield Beach, FL, 1987; pp 665–694.

(12) Mathey, F. *Chem. Rev.* **1988**, *88*, 429.

(13) Mathey, F. *Angew. Chem., Int. Ed. Engl.* **1987**, *26*, 275.

(14) (a) Mathey, F.; Mercier, F. *Tetrahedron Lett.* **1981**, *22*, 319. (b) Marinetti, A.; Mathey, F.; Fischer, J.; Mitschler, A. *J. Chem. Soc., Chem. Commun.* **1982**, 667.

(15) Jeffrey, J. C.; Rauchfuss, T. B. *Inorg. Chem.* **1979**, *18*, 2658.

$H{=}CH_2$, $PhSCH{=}CH_2$, $PhS(O)CH{=}CH_2$, $PhS(O)_2CH{=}CH_2$, $Me_2NC(O)CH{=}CH_2$, $N{\equiv}CCH{=}CH_2$, $N(CH_2C(CH_3){=}CH_2)_3$, and $C_2H_5OCH{=}CH_2$ (Aldrich), and $Ph_2PCH{=}CH_2$, $PhP(CH{=}CH_2)_2$, $PhP(CH_2CH{=}CH_2)_2$, $P(OCH_2CH{=}CH_2)_3$, and $P(C{\equiv}CPh)_3$ (Organometallics, Inc.) were used as received. DMPP,[16] $[(\eta^5\text{-}C_5H_5)Ru(CH_3CN)_3]PF_6$,[17] $[(\eta^6\text{-}C_6H_6)RuCl_2]_2$,[18] $[(\eta^6\text{-}C_6H_6)Ru(\eta^5\text{-}C_5H_5)]Cl$,[19] $[(\eta^6\text{-}C_6H_6)Ru(\eta^5\text{-}C_5H_5)]PF_6$,[17] and $(\eta^5\text{-}C_5H_5)Ru(Ph_3P)_2Cl$[20] were prepared by literature procedures. Silica gel used for chromatography (grade 12, 28–200 mesh) was obtained from Aldrich. All preparations involving phosphines were carried out under a dry nitrogen atmosphere. Melting points were determined on a Mel-Temp apparatus and are uncorrected. Elemental analyses were performed by Galbraith Laboratories, Knoxville, TN 37921. Infrared spectra were obtained on a Perkin-Elmer 599 spectrometer. Cyclic voltammograms were recorded as previously described.[21] $^{31}P\{^1H\}$ NMR spectra were recorded at 40.26 MHz on a JEOL FX-100 spectrometer in the FT mode or at 121.65 MHz on a General Electric GN-300 spectrometer. Phosphorus chemical shifts are relative to internal PF_6^- (−144.95 ppm) with a positive value being downfield of the reference. The ^1H, $^1H\{^{31}P\}$, $^{13}C\{^1H\}$, and carbon attached proton test (APT) spectra were recorded at 300, 300, 75, and 75 MHz, respectively, on a General Electric GN-300 spectrometer. Proton and carbon chemical shifts are relative to internal $(CH_3)_4Si$, $CDCl_3$, or CD_3NO_2. Positive values are downfield of the reference.

B. Synthesis. (Acetonitrile)(η^5-cyclopentadienyl)bis(1-phenyl-3,4-dimethylphosphole)ruthenium(II) Hexafluorophosphate (1). Under a purge of dry nitrogen, DMPP (0.50 mL, 2.66 mmol) was added by syringe to a stirred red-orange solution of $[(\eta^5\text{-}C_5H_5)Ru(CH_3CN)_3]PF_6$ (0.50 g, 1.15 mmol) in 20 mL of acetonitrile. The solution color lightened immediately. The flask was stoppered with a septum under N_2, and the mixture was stirred with a magnetic stirring bar at ambient temperature overnight. Removal of the solvent on a rotary evaporator gave an orange oil, which was washed with anhydrous diethyl ether (3 × 5 mL) and eluted through a short silica gel column with dichloromethane. The eluate was evaporated to dryness on a rotary evaporator, and the residue was dried under vacuum overnight to give a yellow solid (0.80 g, 95%): mp 74 °C dec. IR (KBr): ν_{CN} 2280 cm^{-1}. $^{31}P\{^1H\}$ NMR ($CDCl_3$): δ 45.09 (s, 2 P, DMPP), −144.95 (septet, $^1J(PF)$ = 713 Hz, PF_6^-). ^1H NMR ($CDCl_3$): δ 1.95 (s, 6 H, CH_3), 2.02 (s, 6 H, CH_3), 2.11 (t, $^5J(PH)$ = 1.5 Hz, 3 H, CH_3CN), 4.77 (s, 5 H, C_5H_5), 6.33 (m, $|^2J(PH) + {}^4J(PH)|$ = 35.12 Hz, 4 H, H_α), 7.0–7.6 (m, 10 H, Ph). $^{13}C\{^1H\}$ NMR ($CDCl_3$): δ 3.54 (s, *CH_3*CN), 17.28 (T, $|^3J(PC) + {}^5J(PC)|$ = 11.71 Hz, CH_3), 17.36 (T, $|^3J(PC) + {}^5J(PC)|$ = 11.94 Hz, CH_3), 79.62 (s, C_5H_5), 126.14 (s, CH_3*CN*), 128.45 (T, $|^1J(PC) + {}^3J(PC)|$ = 47.00 Hz, C_α), 128.45 (T, $|^3J(PC) + {}^5J(PC)|$ = 10.20 Hz, C_m), 128.77 (T, $|^1J(PC) + {}^3J(PC)|$ = 47.00 Hz, C_α), 129.29 (m, C_i), 129.94 (s, C_p), 131.43 (T, $|^2J(PC) + {}^4J(PC)|$ = 10.95 Hz, C_o), 149.09 (T, $|^2J(PC) + {}^4J(PC)|$ = 9.30 Hz, C_β), 150.73 (T, $|^2J(PC) + {}^4J(PC)|$ = 8.18 Hz, C_β). Anal. Calcd for $C_{31}H_{34}F_6NP_3Ru$: C, 51.10; H, 4.70. Found: C, 51.47; H, 4.84.

(Acetonitrile)(η^5-cyclopentadienyl)bis(vinyldiphenylphosphine)ruthenium(II) Hexafluorophosphate (2). Similarly, from 0.50 g (1.15 mmol) of $[(\eta^5\text{-}C_5H_5)Ru(CH_3CN)_3]PF_6$ and 0.60 mL (2.51 mmol) of $Ph_2PCH{=}CH_2$ were obtained 0.876 g (99.9%) of yellow crystals of **2**; mp 170–171 °C. IR (KBr): ν_{CN} 2300 cm^{-1}. $^{31}P\{^1H\}$ NMR ($CDCl_3$): δ 39.84 (s, 2 P, $Ph_2PCH{=}CH_2$), −144.95 (septet, $^1J(PF)$ = 716 Hz, 1 P, PF_6^-). ^1H NMR ($CDCl_3$): δ 2.36 (t, $^5J(PH)$ = 1.50 Hz, 3 H, CH_3CN), 4.62 (s, 5 H, C_5H_5), 5.07 (ddd, $^3J(PH)$ = 17.73, $^3J(ac)$ = 17.73, $^2J(bc)$ = 1.80 Hz, 2 H, H_c), 5.72 (ddd, $^2J(PH)$ = 24.04, $^3J(ac)$ = 17.73, $^3J(ab)$ = 12.32, 2 H, H_a), 5.79 (ddd, $^3J(PH)$ = 36.97, $^3J(ab)$ = 12.32, $^2J(bc)$ = 1.80 Hz, 2 H, H_b), 6.9–7.6 (m, 20 H, Ph). $^{13}C\{^1H\}$ NMR ($CDCl_3$) δ 4.33 (s, *CH_3*CN), 82.59 (t, $^2J(PC)$ = 1.66 Hz, C_5H_5), 127.88 (s, CH_3*CN*), 128.36 (T, $|^3J(PC) + {}^5J(PC)|$ = 9.75 Hz, C_m), 128.61 (T, $|^3J(PC) + {}^5J(PC)|$ = 9.98 Hz, C_m), 128.99 (s, C_β), 130.07 (s, C_p), 130.81 (s, C_p), 132.05 (five lines, $^1J(PC)$ = 40.23, $^3J(PC)$ = −1.54, $^2J(PP)$ = 36.82 Hz, C_α), 133.22 (T, $|^2J(PC) + {}^4J(PC)|$ = 10.13 Hz, C_o), 132.92 (five lines, $^1J(PC)$ = 44.76, $^3J(PC)$ = 4.5, $^2J(PP)$ = 36.82 Hz, C_i), 133.92 (T, $|^2J(PC) + {}^4J(PC)|$ = 11.19 Hz, C_o), 135.52 (five lines, $^1J(PC)$ = 44.76, $^3J(PC)$ = 4.5, $^2J(PP)$ = 36.82 Hz, C_i), Anal. Calcd for $C_{35}H_{34}F_6NP_3Ru$: C, 54.15; H, 4.38; N, 1.80. Found: C, 53.90, 53.80; H, 4.40, 4.30; N, 1.90, 1.90.

(Acetonitrile)(η^5-cyclopentadienyl)bis(divinylphenylphosphine)ruthenium(II) Hexafluorophosphate (3). Similarly, from 0.50 g (1.15 mmol) of $[(\eta^5\text{-}C_5H_5)Ru(CH_3CN)_3]PF_6$ and 0.60 mL (2.51 mmol) of $PhP(CH{=}CH_2)_2$ were obtained 0.777 g (99.9%) of yellow crystals of **3**; mp 144–145 °C. $^{31}P\{^1H\}$ NMR ($CDCl_3$): δ 32.41 (s, 2 P, $PhP(CH{=}CH_2)_2$), −144.95 (septet, $^1J(PF)$ = 716 Hz, 1 P, PF_6). ^1H NMR ($CDCl_3$): δ 2.31 (t, $^5J(PH)$ = 1.50 Hz, 3 H, CH_3CN), 4.65 (s, 5 H, C_5H_5), 5.23 (ddd, $^3J(PH)$ = 18.93, $^3J(ac)$ = 18.03, $^2J(bc)$ = 1.20 Hz, 2 H, H_c), 5.63 (ABX, $^3J(PH)$ = 18.93, $^3J(a'c')$ = 18.16, $^2J(b'c')$ = 1.32 Hz, 2 H, $H_{c'}$), 5.87 (ddd, $^3J(PH)$ = 36.66, $^3J(ab)$ = 12.02, $^2J(bc)$ = 1.20 Hz, 2 H, H_b), 6.05 (ABX, $^2J(PH)$ = 24.82, $^3J(a'c')$ = 18.16, $^3J(a'b')$ = 11.90 Hz, 2 H, $H_{a'}$), 6.06 (ABX, $^3J(PH)$ = 28.98, $^3J(a'b')$ = 11.90, $^2J(b'c')$ = 1.32 Hz, 2 H, $H_{b'}$), 6.23 (ddd, $^2J(PH)$ = 24.04, $^3J(ac)$ = 18.03, $^3J(ab)$ = 12.02 Hz, 2 H, H_a), 7.3–7.5 (m, 10 H, Ph). $^{13}C\{^1H\}$ NMR ($CDCl_3$): δ 4.22 (s, *CH_3*CN), 81.68 (t, $^2J(PC)$ = 1.89 Hz, C_5H_5), 127.53 (s, CH_3*CN*), 128.58 (T, $|^3J(PC) + {}^5J(PC)|$ = 9.82 Hz, C_m), 129.03 (s, C_p), 130.51 (s, C_β), 130.74 (s, C_β), 132.35 (five lines, $^1J(PC)$ = 39.66, $^2J(PP)$ = 39.14, $^3J(PC)$ = 3.87 Hz, C_α), 132.53 (T, $|^2J(PC) + {}^4J(PC)|$ = 10.81 Hz, C_o), 132.67 (five lines, $^2J(PP)$ = 39.14, $^1J(PC)$ = 29.30, $^3J(PC)$ = 3.68 Hz, C_i), 133.12 (five lines, $^1J(PC)$ = 41.52, $^2J(PP)$ = 39.14, $^2J(PC)$ = 1.78 Hz, C_α). Anal. Calcd for $C_{27}H_{30}F_6NP_3Ru$: C, 47.96; H, 4.44; N, 2.07. Found: C, 48.10, 47.90; H, 4.30, 4.30; N, 1.80, 1.90.

Intramolecular [4 + 2] Cycloaddition of $[(\eta^5\text{-}C_5H_5)Ru(DMPP)_2(DPVP)]PF_6$ (4a,b). To a yellow solution of **1** (1.0 g, 1.37 mmol) in 50 mL of 1,2-dichloroethane was added DPVP (0.4 mL, 1.67 mmol) by a syringe under a purge of N_2. The solution was refluxed under N_2 overnight, after which the solvent was removed on a rotary evaporator and the residue was washed with anhydrous diethyl ether (3 × 10 mL). Two products (**4a,b**) were obtained. They were separated by fractional crystallization from CH_2Cl_2/ether at low temperature. The less soluble major product, a needlelike yellow crystalline solid, crystallized out of solution first. The more soluble product, a blocklike yellow crystalline solid, crystallized out of solution later. The isolated ratio of the two products is 5:1. The overall isolated yield was 87.6%: mp 176 °C (**4a**), 180–183 °C (**4b**). The $^{31}P\{^1H\}$ NMR data are given in Table I. ^1H NMR: **4b** (CD_3NO_2), δ 1.51 (apparent t, $^4J(PH)$ = $^4J(HH)$ = 1.05 Hz, 3 H, 5-CH_3), 1.60 (s, 3 H, 6-CH_3), 1.80 (apparent t, $^4J(PH)$ = $^4J(HH)$ = 1.05 Hz, 3 H, β-CH_3), 2.04 (apparent t, $^4J(PH)$ = $^4J(HH)$ = 1.05 Hz, 3 H, β-CH_3), 1.88 (m, $^3J(PH)$ = 28.0, $^2J(H_3H_4)$ = 13.36, $^3J(H_2H_4)$ = 2.00 Hz, 1 H, H_4), 2.42 (dddd, $^3J(PH)$ = 22.7, $^3J(PH)$ = 3.00, $^2J(H_3H_4)$ = 13.36, $^2J(H_2H_3)$ = 8.01 Hz, 1 H, H_3), 2.61 (apparent q, $^2J(PH)$ = $^3J(PH)$ = $^4J(H_1H_5)$ = 1.95 Hz, 1 H, H_1), 3.05 (dddd, $^3J(PH)$ = 39.07, $^2J(PH)$ = 8.01, $^3J(H_2H_3)$ = 8.01, $^3J(H_2H_4)$ = 2.00 Hz, 1 H, H_2), 3.56 (t, $^2J(PH)$ = $^4J(H_1H_5)$ = 1.95 Hz, 1 H, H_5), 4.78 (s, 5 H, C_5H_5), 6.12 (dq, $^2J(PH)$ = 28.85, $^4J(HH)$ = 1.05 Hz, 1 H, H_α), 6.24 (dq, $^2J(PH)$ = 29.45, $^4J(HH)$ = 1.05 Hz, 1 H, H_α), 7.3–7.7 (m, 20 H, Ph); **4a** ($CDCl_3$), δ 1.25 (s, 3 H, 5-CH_3), 1.38 (s, 3 H, 6-CH_3), 1.87 (s, 3 H, β-CH_3), 1.89 (s, 3 H, β-CH_3), 2.03 (m, $^3J(PH)$ = 22.24, $^2J(H_3H_4)$ = 12.62, $^3J(H_2H_4)$ = 1.8 Hz, 1 H, H_4), 2.20 (dddd, $^3J(PH)$ = 22.54, $^3J(PH)$ = 3.00, $^2J(H_3H_4)$ = 12.62, $^2J(H_2H_3)$ = 8.11 Hz, 1 H, H_3), 2.84 (d, $^2J(PH)$ = 1.2 Hz, 1 H, H_1), 2.90 (bs, 1 H, H_5), 3.34 (apparent ddt, $^3J(PH)$ = 40.87, $^2J(PH)$ = 8.11, $^3J(H_2H_3)$ = 8.11, $^3J(H_2H_4)$ = 1.8 Hz, 1 H, H_2), 4.99 (d, $^2J(PH)$ = 34.56 Hz, 1 H, H_α), 5.13 (s, 5 H, C_5H_5), 5.56 (d, $^2J(PH)$ = 35.76 Hz, 1 H, H_α), 6.9–7.5 (m, 20 H, Ph). $^{13}C\{^1H\}$ NMR: **4a** ($CDCl_3$), δ 13.56 (d, $^3J(PC)$ = 2.57 Hz, 5-CH_3), 15.35 (d, $^3J(PC)$ = 3.93 Hz, 6-CH_3), 16.47 (d, $^3J(PC)$ = 11.87 Hz, β-CH_3), 17.65 (d, $^3J(PC)$ = 11.86 Hz, β-CH_3), 31.39 (dd, $^1J(PC)$ = 41.3 Hz, $^2J(PC)$ = 33.6 Hz, C_2), 32.47 (dd, $^2J(PC)$ = 16.3, $^2J(PC)$ = 5.5 Hz, C_3), 54.09 (dd, $^1J(PC)$ = 35.2, $^2J(PC)$ = 11.8 Hz, C_1), 54.81 (d, $^1J(PC)$ = 28.64 Hz, C_4), 83.29 (s, C_5H_5), 128.01 (d, $^3J(PC)$ = 9.22 Hz, C_m), 128.53 (d, $^3J(PC)$ = 10.42 Hz, C_m), 128.57 (d, $^1J(PC)$ = 55.01 Hz, C_α), 128.58 (d, $^3J(PC)$ = 9.52 Hz, C_m), 129.12 (d, $^3J(PC)$ = 9.60 Hz, C_m), 129.88 (d, $^4J(PC)$ = 1.51 Hz, C_p), 129.97 (d, $^4J(PC)$ = 2.04 Hz, C_p), 130.21 (d, $^4J(PC)$ = 1.96 Hz, C_p), 130.40 (d, $^4J(PC)$ = 1.66 Hz, C_p), 130.21 (d, $^2J(PC)$

(16) Breque, A.; Mathey, F.; Savignac, P. *Synthesis* **1981**, 983.
(17) Gill, T. P.; Mann, K. R. *Organometallics* **1982**, *1*, 485.
(18) Zelonka, R. A.; Baird, M. C. *Can. J. Chem.* **1972**, *50*, 3063.
(19) Zelonka, R. A.; Baird, M. C. *J. Organomet. Chem.* **1972**, *44*, 383.
(20) Bruce, M. I.; Windsor, N. J. *Aust. J. Chem.* **1977**, *30*, 1601.
(21) Milosavljević, E. B.; Solujić, L.; Krassowski, D. W.; Nelson, J. H. *J. Organomet. Chem.* **1988**, *352*, 177.

Table I. 121.65-MHz $^{31}P\{^1H\}$ NMR Data[a] for the Complexes

		$\delta^{31}P$ (m),[c] ppm			$^2J(PP)$, Hz		
compd no.	ratio[b]	P_1	P_2	P_3	P_1P_2	P_2P_3	P_1P_3
4a	5	151.18 (dd)	54.16 (dd)	48.84 (dd)	41.24	34.55	30.30
4b	1	152.47 (dd)	69.57 (dd)	40.21 (dd)	48.83	39.06	26.90
5a	3	151.50 (dd)	56.01 (dd)	40.56 (dd)	53.71	46.10	37.83
5b	1	154.71 (dd)	60.19 (dd)	47.84 (dd)	48.83	46.39	39.06
5c	4	159.20 (d)	78.60 (t)		43.94		
6a	9	151.08 (dd)	52.18 (dd)	42.18 (dd)	39.42	37.29	31.51
6b	1	152.35 (dd)	68.96 (dd)	61.83 (dd)	46.23	40.63	23.48
7a	6	151.99 (dd)	48.44 (dd)	35.24 (dd)	43.95	34.18	34.18
7b	1	154.65 (dd)	45.78 (dd)	39.48 (dd)	43.95	34.18	34.18
8			44.08 (d)	23.61 (t)	39.06		
9a	3	129.46 (dd)	44.51 (dd)	17.26 (dd)	34.18	29.30	43.95
9b	1	123.72 (dd)	47.95 (dd)	13.33 (dd)	29.30	39.07	48.83
9c	1	127.57 (AB)	125.19 (AB)	6.13 (X)	31.23	43.15	44.20
9d		124.11 (d)	6.51 (t)		45.56		
10		152.90 (d)		46.08 (t)			34.18
11	*d*	160.83 (bs)		45.29 (d)			39.06
11a	3[e]	164.81 (d)		44.69 (d)			35.41
11b	1[e]	159.41 (d)		46.50 (d)			35.41
12		159.25 (d)		67.09 (d)			39.06
13a	3	154.65 (dd)	50.01 (dd)	41.36 (dd)	34.18	29.30	43.94
13b	2	156.83 (dd)	45.53 (dd)	42.45 (dd)	34.18	34.18	43.94
14			48.49 (AB)	46.57 (AB)			43.95
15			43.43 (AB)	37.92 (AB)			43.94
16			147.60 (t)	44.80 (d)			58.60
17			43.11 (d)	29.20 (d)			39.06
18				46.00 (s)			
19				46.03 (s)			
20				46.36 (s)			
21				44.93 (s)			

[a] **4a,b**, **5a–c**, **6a,b**, **7a–d**, and 8 in CD_3NO_2, the other complexes in $CDCl_3$. [b] The ratio is among stereoisomers of the same composition. [c] Abbreviations: m, multiplicity; bs, broad singlet; d, doublet; dd, doublet of doublets; t, triplet; AB, AB quartet, X, X part of ABX. [d] At 25 °C, averaged spectrum. [e] At −20 °C in $CDCl_3$, stopped exchange limit.

= 10.42 Hz, C_o), 130.74 (d, $^2J(PC)$ = 10.05 Hz, C_o), 131.50 (d, $^2J(PC)$ = 10.28 Hz, C_o), 131.50 (dd, $^1J(PC)$ = 54.9, $^3J(PC)$ = 2.3 Hz, C_α), 131.65 (d, $^2J(PC)$ = 12.55 Hz, C_o), 136.43 (d, $^1J(PC)$ = 35.82 Hz, C_i), 136.46 (d, $^1J(PC)$ = 36.27 Hz, C_i), 137.22 (s, C_5 and C_6), 137.22 (d, $^1J(PC)$ = 43.0 Hz, 2 C_i), 146.88 (d, $^2J(PC)$ = 7.86 Hz, C_β), 153.10 (d, $^2J(PC)$ = 9.07 Hz, C_β); **4b** (CD_3NO_2), 13.94 (d, $^2J(PC)$ = 2.34 Hz, 5-CH_3), 14.94 (d, $^2J(PC)$ = 0.60 Hz, 6-CH_3), 17.46 (d, $^3J(PC)$ = 11.94 Hz, β-CH_3), 17.92 (d, $^3J(PC)$ = 11.64 Hz, β-CH_3), 32.78 (dd, $^2J(PC)$ = 15.1, $^2J(PC)$ = 2.1 Hz, C_3), 33.40 (dd, $^1J(PC)$ = 37.3, $^2J(PC)$ = 30.9 Hz, C_2), 50.74 (dd, $^1J(PC)$ = 28.9, $^3J(PC)$ = 2.0 Hz, C_4), 60.54 (dd, $^1J(PC)$ = 35.3, $^2J(PC)$ = 15.6 Hz, C_1), 85.84 (q, $^2J(PC)$ = 1.74 Hz, C_5H_5), 129.81 (d, $^3J(PC)$ = 9.52 Hz, C_m), 129.83 (d, $^3J(PC)$ = 10.05 Hz, C_m), 129.87 (d, $^3J(PC)$ = 9.37 Hz, C_m), 130.08 (d, $^3J(PC)$ = 10.20 Hz, C_m), 130.83 (d, $^1J(PC)$ = 45.12 Hz, C_α), 131.28 (d, $^4J(PC)$ = 2.72 Hz, C_p), 131.32 (d, $^4J(PC)$ = 2.83 Hz, C_p), 131.39 (d, $^4J(PC)$ = 2.68 Hz, C_p), 132.11 (d, $^4J(PC)$ = 1.74 Hz, C_p), 132.31 (d, $^1J(PC)$ = 45.12 Hz, C_α), 132.31 (d, $^2J(PC)$ = 8.99 Hz, C_o), 132.70 (d, $^2J(PC)$ = 9.82 Hz, C_o), 133.07 (d, $^2J(PC)$ = 11.03 Hz, C_o), 136.75 (d, $^2J(PC)$ = 11.49 Hz, C_o), 136.80 (dd, $^1J(PC)$ = 45.0, $^3J(PC)$ = 2.7 Hz, C_i), 136.87 (dd, $^1J(PC)$ = 38.9, $^3J(PC)$ = 3.02 Hz, 2 C_i), 139.54 (s, C_5), 139.58 (s, C_6), 150.83 (d, $^2J(PC)$ = 8.46 Hz, C_β), 153.13 (d, $^2J(PC)$ = 8.84 Hz, C_β). Anal. Calcd for $C_{43}H_{44}F_6P_4Ru \cdot 0.5CH_2Cl_2$: C, 55.45; H, 4.81. Found for **4a**: C, 56.01; H, 4.09. Found for **4b**: C, 55.21; H, 5.03.

Intramolecular [4 + 2] Cycloaddition of $[(\eta^5\text{-}C_5H_5)Ru(DMPP)_2(DVPP)]PF_6$ (5a–c). A mixture containing 0.73 g (1 mmol) of **1** and 0.25 mL (1.44 mmol) of DVPP in 50 mL of 1,2-dichloroethane was refluxed under an N_2 atmosphere for 20 h to produce a colorless precipitate and a yellow solution. The mixture was cooled to room temperature, and the colorless product (**5c**) was isolated by filtration and washed with chloroform and anhydrous diethyl ether, yielding the first crop (0.35 g) of **5c**. The filtrate was evaporated to dryness, the residue was dissolved in chloroform, and a second crop (0.05 g) of **5c** precipitated and was isolated by filtration. A $^{31}P\{^1H\}$ NMR spectrum showed that the filtrate contained **5a,b** in a 3:1 ratio. **5a,b** could not be separated and isolated. The two crops of **5c** were combined, recrystallized from $CH_3NO_2/CH_2Cl_2/Et_2O$, and dried in vacuo, affording 0.35 g (41.4%) of colorless crystals: mp 328–329 °C. ^1H NMR (DMSO-d_6): δ 1.27 (m, $^3J(PH)$ = 30.0, $^2J(H_3H_4)$ = 12.60 Hz, 2 H, H_4), 1.29 (s, 6 H, 5-CH_3), 1.62 (s, 6 H, 6-CH_3), 1.70 (dddd, $^3J(PH)$ = 23.1, $^2J(H_3H_4)$ = 12.6, $^3J(H_2H_3)$ = 6.9, $^3J(PH)$ = 3.7 Hz, 2 H, H_3), 2.77 (bs, 2 H, H_1), 3.03 (apparent dt, $^3J(PH)$ = 40.15, $^2J(PH)$ = $^3J(H_2H_3)$ = 6.9 Hz, 2 H, H_2), 3.66 (bs, 2 H, H_5), 5.14 (s, 5 H, C_5H_5), 7.2–8.0 (m, 15 H, Ph). $^{13}C\{^1H\}$ NMR (DMSO-d_6) δ 13.28 (s, 5-CH_3), 14.92 (s, 6-CH_3), 33.10 (dT, $|^2J(PC) + {}^4J(PC)|$ = 11.6, $^2J(PC)$ = 7.9 Hz, C_2), 35.1 (m, C_2), 51.91 (d five lines, $|^1J(PC) + {}^3J(PC)|$ = 16.9, $^2J(PC)$ = 15.1 Hz, C_1), 53.1 (d five lines, $|^1J(PC) + {}^3J(PC)|$ = 24.1, $^3J(PC)$ = 16.5 Hz, C_4), 82.01 (s, C_5H_5), 127.75 (T, $|^3J(PC) + {}^5J(PC)|$ = 7.86 Hz, C_m), 128.85 (d, $^3J(PC)$ = 10.05 Hz, $C_{m'}$), 129.49 (s, C_p), 130.76 (T, $|^2J(PC) + {}^4J(PC)|$ = 7.94 Hz, C_o), 130.94 (s, C_p), 132.52 (d, $^1J(PC)$ = 46.40 Hz, $C_{i'}$), 133.51 (d, $^2J(PC)$ = 9.52 Hz, $C_{o'}$), 134.54 (d five lines, $|^1J(PC) + {}^3J(PC)|$ = 37.79, $^4J(PC)$ = 3.24 Hz, $C_{i'}$), 137.18 (s, C_5), 137.21 (s, C_6). Anal. Calcd for $C_{39}H_{42}F_6P_4Ru$: C, 55.15; H, 4.94. Found: C, 54.90, 54.80; H, 4.50, 4.70.

Intramolecular [4 + 2] Cycloaddition of $[(\eta^5\text{-}C_5H_5)Ru(DMPP)(DPVP)_2]PF_6$ (6a,b). These two complexes were prepared in the same manner as **4a,b** by reaction of **2** (1.00 g, 1.29 mmol) with DMPP (0.30 mL, 1.60 mmol). They were formed in an about 9:1 ratio and were separated by chromatography on a silica gel column with CH_2Cl_2. The first yellow band to elute from the column contained only the major product **6a**. The second band contained the minor product **6b** and other unidentified products, which were not further separated. **6a** was crystallized from CH_2Cl_2/Et_2O at low temperature. The light yellow crystalline solid was isolated by filtration and dried in vacuo (1.01 g, 84.9%): mp 267 °C dec. ^1H NMR (CD_3NO_2): δ 1.53 (s, 3 H, 5-CH_3), 1.98 (s, 3 H, 6-CH_3), 2.05–2.27 (m, 2 H, H_3, H_4), 3.16 (bs, 1 H, H_1), 3.59 (bs, 1 H, H_5), 3.62 (apparent dt, $^3J(PH)$ = 41.34, $^2J(PH)$ = $^3J(H_2H_3)$ = 9.18 Hz, 1 H, H_2), 4.55 (apparent t, $^3J(PH)$ = $^3J(H_aH_c)$ = 17.11 Hz, 1 H, H_c), 5.05 (s, 5 H, C_5H_5), 5.54 (ddd, $^2J(PH)$ = 29.57, $^3J(H_aH_c)$ = 17.11, $^3J(H_aH_b)$ = 12.01 Hz, 1 H, H_a), 5.86 (dd, $^3J(PH)$ = 35.12, $^3J(H_aH_b)$ = 12.01 Hz, 1 H, H_b), 5.97–7.90 (m, 25 H, Ph). $^{13}C\{^1H\}$ NMR (CD_3NO_2): δ 13.80 (d, $^3J(PC)$ = 1.89 Hz, 5-CH_3), 15.28 (s, 6-CH_3), 32.54 (dd, $^1J(PC)$ = 40.3, $^2J(PC)$ = 33.6 Hz, C_2), 33.36 (dd, $^2J(PC)$ = 15.0, $^2J(PC)$ = 5.4 Hz, C_3), 55.2 (dd, $^1J(PC)$ = 33.80, $^2J(PC)$ = 10.95 Hz, C_1), 56.37 (d, $^1J(PC)$ = 31.52 Hz, C_4), 85.79 (s, C_5H_5), 129.04 (d, $^3J(PC)$ = 9.90 Hz, C_m), 129.62 (d, $^3J(PC)$ = 9.14 Hz, C_m), 129.83 (d, $^3J(PC)$ = 9.60 Hz,

C_m), 130.12 (d, ^3J(PC) = 9.67 Hz, 2 C_m), 130.36 (s, C_p), 130.66 (s, C_p), 131.20 (s, C_p), 131.48 (s, C_p), 131.50 (s, C_β), 131.92 (d, ^2J(PC) = 9.52 Hz, C_o), 132.73 (d, ^2J(PC) = 8.62 Hz, C_o), 133.23 (d, ^2J(PC) = 10.35 Hz, C_o), 133.49 (d, ^2J(PC) = 8.46 Hz, C_o), 134.17 (d, ^1J(PC) = 33.40 Hz, C_α), 135.56 (d, ^2J(PC) = 10.73 Hz, C_o), 137.14 (d, ^1J(PC) = 34.08 Hz, C_i), 137.16 (d, ^1J(PC) = 33.70 Hz, C_i), 137.20 (d, ^1J(PC) = 34.01 Hz, C_i), 137.99 (d, ^1J(PC) = 48.97 Hz, C_i), 138.02 (d, ^1J(PC) = 48.51 Hz, C_i), 139.20 (s, C_5), 139.79 (s, C_6). Anal. Calcd for $C_{45}H_{44}F_6P_4Ru$: C, 58.51; H, 4.80. Found: C, 58.52; H, 4.85.

Intramolecular [4 + 2] Cycloaddition of [(η^5-C_5H_5)Ru(DMPP)(DVPP)$_2$]PF_6 (7a,b). These two compounds were prepared similarly. Complex **3** was reacted with DMPP in a 1:1.1 molar ratio in 1,2-dichloroethane at 80 °C for 10 h. A $^{31}P\{^1H\}$ NMR spectrum of the crude reaction mixture showed quantitative conversion of **3** to **7a,b** in a 6:1 ratio. They are not separable by either chromatography or fractional crystallization from a variety of solvent mixtures: e.g. CH_2Cl_2/Et_2O, $CHCl_3/Et_2O$, or $CHCl_3$/petroleum ether. They were characterized only by their $^{31}P\{^1H\}$ NMR spectra.

(η^5-Cyclopentadienyl)(diallylphenylphosphine)bis(1-phenyl-3,4-dimethylphosphole)ruthenium(II) Hexafluorophosphate (8). To a solution containing (0.50 g, 0.685 mmol) of **1** in 30 mL of 1,2-dichloroethane was added 0.20 mL (0.90 mmol) of DAPP by a syringe under N_2. After the mixture was heated at reflux for 20 h, the solvent was removed on a rotary evaporator, the residue was washed with anhydrous diethyl ether (5 × 10 mL), and the solid was dried under vacuum overnight: yield 0.60 g (99.9%) of yellow solid. ^1H NMR ($CDCl_3$): δ 1.90 (s, 6 H, CH_3), 1.91 (s, 6 H, CH_3), 2.54–2.80 (m, 4 H, CH_2), 5.1 (m, 4 H, =CH_2), 5.4 (m, 2 H, =CH), 5.15 (s, 5 H, C_5H_5), 6.02 (m, $|^2J$(PH) + ^4J(PH)| = 34.86 Hz, 2 H, H_α), 6.21 (m, $|^2J$(PH) + ^4J(PH)| = 33.96 Hz, 2 H, H_α), 6.75–7.60 (m, 15 H, Ph). $^{13}C\{^1H\}$ NMR: δ 17.13 (T, $|^3J$(PC) + ^5J(PC)| = 11.26 Hz, β-CH_3), 17.26 (T, $|^3J$(PC) + ^5J(PC)| = 11.33 Hz, β-CH_3), 35.00 (d, ^1J(PC) = 25.85 Hz, CH_2), 82.98 (s, C_5H_5), 119.94 (d, ^3J(PC) = 10.28 Hz, C_b), 128.04 (d, ^3J(PC) = 8.92 Hz, $C_{m'}$), 128.57 (T, $|^3J$(PC) + ^5J(PC)| = 9.75 Hz, C_m), 129.78 (s, $C_{p'}$), 129.98 (D, $|^1J$(PC) + ^3J(PC)| = 30.23 Hz, C_α), 130.07 (s, C_p), 130.52 (d, ^2J(PC) = 7.48 Hz, $C_{o'}$), 130.60 (d, ^2J(PC) = 6.80 Hz, C_β), 131.06 (T, $|^2J$(PC) + ^4J(PC)| = 10.58 Hz, C_o), 131.09 (D, $|^1J$(PC) + ^3J(PC)| = 29.93 Hz, C_α), 132.01 (m, C_i), 136.30 (m, $C_{i'}$), 150.03 (T, $|^2J$(PC) + ^4J(PC)| = 7.94 Hz, C_β), 150.24 (T, $|^2J$(PC) + ^4J(PC)| = 8.84 Hz, C_β). The primed carbons are the phenyl carbons of DAPP. Anal. Calcd for $C_{41}H_{46}F_6P_4Ru$: C, 56.13; H, 5.24. Found: C, 56.02; H, 5.18.

Intramolecular [4 + 2] Cycloaddition of 8 (9a–c). An orange solution of **8** (0.50 g, 0.57 mmol) in 30 mL of 1,2-dichloroethane was heated at reflux for 48 h under N_2. A $^{31}P\{^1H\}$ NMR spectrum of the crude reaction mixture showed quantitative conversion to **9a–c** (in a 4:2:1 ratio). They were separated by a combination of chromatography on silica gel (CH_2Cl_2) and fractional crystallization from CH_2Cl_2/Et_2O. Purification of **9c** was accomplished by crystallization from $CH_3NO_2/CH_2Cl_2/Et_2O$. On one occasion another bis-Diels–Alder product, **9d**, was observed in trace amounts by $^{31}P\{^1H\}$ NMR spectroscopy (δ(^{31}P) 124.11 (d), 6.51 (t) ppm (^2J(PP) = 45.56 Hz), −144.95 (septet, ^1J(PF) = 714 Hz)). Mp: **9a**, 178–180 °C; **9c**, 328–330 °C. ^1H NMR (CD_3NO_2): **9a**, δ 1.29 (apparent t, ^4J(HH) = ^4J(PH) = 0.90 Hz, 3 H, β-CH_3), 1.60 (apparent t, ^4J(HH) = ^4J(PH) = 1.20 Hz, 3 H, β-CH_3), 1.70 (apparent t, ^4J(HH) = ^4J(PH) = 1.35 Hz, 3 H, CH_3), 2.05–2.25 (m, 2 H, H_3, H_4), 2.14 (bs, 3 H, CH_3), 2.48 (ddd, ^2J(HH) = 14.13, ^2J(PH) = 9.02 Hz, ^3J(HH) = 3.90 Hz, 1 H, PCH_2), 2.68–3.04 (m, 3 H, H_2 and PCH_2), 2.81 (m, 1 H, H_5), 2.84 (ddd, ^2J(HH) = 14.13, ^2J(PH) = 9.32, ^3J(HH) = 4.50 Hz, 1 H, PCH_2), 2.95 (m, 1 H, H_1), 4.85–5.02 (m, 2 H, H_a and H_b), 4.90 (s, 5 H, C_5H_5), 5.20–5.36 (m, 1 H, H_c), 5.93 (dq, ^2J(PH) = 36.36 Hz, ^4J(HH) = 0.9 Hz, 1 H, H_α), 6.58 (dq, ^2J(PH) = 36.36 Hz, ^4J(HH) = 0.92 Hz, 1 H, H_α), 7.10–7.65 (m, 15 H, Ph); **9c**, δ 1.27 (apparent t, ^4J(HH) = ^4J(PH) = 1.20 Hz, 3 H, CH_3), 1.47 (apparent t, ^4J(HH) = ^4J(PH) = 1.20 Hz, 3 H, CH_3), 1.62 (apparent t, ^4J(HH) = ^4J(PH) = 1.20 Hz, 3 H, CH_3), 1.80 (apparent t, ^4J(HH) = ^4J(PH) = 1.20 Hz, 3 H, CH_3), 1.90–2.30 (m, 2 H, H_4), 2.75–3.14 (m, 9 H), 3.08 (ddd, ^2J(HH) = 15.02, ^2J(PH) = 7.07, ^3J(HH) = 3.98 Hz, 1 H, PCH_2), 3.24 (m, 1 H, H_5), 3.51 (ddd, ^2J(HH) = 17.13, ^2J(PH) = 12.02, ^3J(HH) = 4.80 Hz, 1 H, PCH_2), 4.25 (s, 5 H, C_5H_5), 5.37–7.9 (m, 15 H, Ph). $^{13}C\{^1H\}$ NMR (CD_3NO_2): **9a**, δ 14.16 (d, ^3J(PC) = 7.48 Hz, CH_3), 17.41 (d, ^3J(PC) = 9.14 Hz, CH_3), 18.05 (d, ^3J(PC) = 7.33 Hz, CH_3), 18.21 (d, ^3J(PC) = 6.95 Hz, CH_3), 33.08 (d, ^1J(PC) = 30.69 Hz, PCH_2), 33.88 (d, ^1J(PC) = 18.44 Hz, PCH_2), 37.20 (d, ^2J(PC) = 25.70 Hz, C_2), 40.47 (dd, ^2J(PC) = 26.83, ^3J(PC) = 7.02 Hz, C_3), 51.30 (dd, ^1J(PC) = 29.63, ^3J(PC) = 6.88 Hz, C_1), 57.24 (d, ^1J(PC) = 30.76 Hz, C_4), 86.44 (d, ^2J(PC) = 6.05 Hz, C_5H_5), 120.49 (d, ^3J(PC) = 8.6 Hz, =CH_2), 128.0–134.0 (m, unresolved Ph, HC=C and C_α), 135.94 (dd, ^1J(PC) = 41.27, ^3J(PC) = 2.65 Hz, C_i), 136.95 (s, C_5), 137.39 (s, C_6), 140.81 (dd, ^1J(PC) = 42.10, ^3J(PC) = 1.21 Hz, C_i), 149.79 (d, ^2J(PC) = 7.78 Hz, C_β), 155.90 (d, ^2J(PC) = 10.66, C_β); **9c**, δ 14.14 (d, ^3J(PC) = 2.08 Hz, CH_3), 14.26 (d, ^3J(PC) = 2.19 Hz, CH_3), 31.11 (d, ^2J(PC) = 19.42 Hz, C_3), 31.72 (d, ^2J(PC) = 19.50 Hz, C_3), 37.69 (d, ^2J(PC) = 33.78 Hz, C_2), 37.96 (d, ^2J(PC) = 35.37 Hz, C_2), 39.05 (d, ^1J(PC) = 28.72 Hz, PCH_2), 41.00 (d, ^1J(PC) = 30.76 Hz, PCH_2), 52.24 (d, ^1J(PC) = 27.06 Hz, C_1), 54.71 (d, ^1J(PC) = 31.36 Hz, C_4), 54.77 (d, ^1J(PC) = 31.31 Hz, C_4), 57.25 (d, ^1J(PC) = 30.30 Hz, C_1), 88.11 (s, C_5H_5), 128–132.4 (unresolved C_o, C_m, C_p), 136.69 (s, C_5), 137.62 (s, C_5), 137.76 (s, C_6), 138.00 (s, C_6), 141.03 (d, ^1J(PC) = 40.74 Hz, C_i), 141.79 (d, ^1J(PC) = 43.53 Hz, C_i), 144.53 (d, ^1J(PC) = 43.76 Hz, C_i). Anal. Calcd for $C_{41}H_{46}F_6P_4Ru$: C, 56.13; H, 5.24. Found for **9a**: C, 55.45; H, 5.12. Found for **9c**: C, 55.60; 55.80; H, 4.90, 4.80.

Intramolecular [4 + 2] Cycloaddition of [(η^5-C_5H_5)Ru(DMPP)$_2$(PhS(O)CH=CH_2)]PF_6 (10). To a yellow-orange solution of **1** (0.50 g, 0.68 mmol) in 30 mL of 1,2-dichloroethane was added 1 mL (7.48 mmol) of PhS(O)CH=CH_2. The solution was heated at reflux under N_2 for 6 h, and the solvent was then removed on a rotary evaporator. Addition of 5 mL of anhydrous diethyl ether produced a yellow crystalline solid, which was isolated by filtration and washed with anhydrous ether. Recrystallization from $CHCl_3$/petroleum ether (60–110 °C) at low temperature yielded 0.50 g (87.7%) of **10**: mp 226 °C dec. IR (KBr): ν_{SO} 1073 cm^{-1}. ^1H NMR ($CDCl_3$): δ 1.46 (s, 6 H, CH_3), 1.83 (s, 3 H, CH_3), 1.94 (s, 3 H, CH_3), 2.02 (ddd, ^3J(PH) = 25.24, ^2J(H_3H_4) = 14.12, ^3J(H_2H_3) = 7.81 Hz, 1 H, H_3), 2.45 (dd, ^2J(H_3H_4) = 14.12, ^3J(H_2H_4) = 3.00 Hz, 1 H, H_4), 3.11 (d, ^2J(PH) = 1.80 Hz, 1 H, H_1), 3.47 (bs, 1 H, H_5), 3.85 (ddd, ^3J(PH) = 39.82, ^3J(H_2H_3) = 7.81, ^3J(H_2H_4) = 3.0 Hz, 1 H, H_2), 5.00 (s, 5 H, C_5H_5), 5.90 (d, ^2J(PH) = 34.26 Hz, 1 H, H_α), 6.65 (d, ^2J(PH) = 32.15 Hz, 1 H, H_α), 7.10–7.90 (m, 15 H, Ph). $^{13}C\{^1H\}$ NMR ($CDCl_3$) δ 13.82 (d, ^3J(PC) = 2.57 Hz, 5-CH_3), 15.29 (d, ^3J(PC) = 1.44 Hz, 6-CH_3), 16.88 (d, ^3J(PC) = 12.55 Hz, β-CH_3), 17.51 (d, ^3J(PC) = 12.77 Hz, β-CH_3), 33.56 (d, ^2J(PC) = 16.10 Hz, C_3), 51.23 (d, ^1J(PC) = 33.94 Hz, C_4), 51.86 (d, ^1J(PC) = 27.96 Hz, C_1), 65.20 (d, ^2J(PC) = 37.03 Hz, C_2), 84.51 (s, C_5H_5), 124.92 (s, $C_{m'}$), 124.99 (d, ^1J(PC) = 45.35 Hz, C_i), 126.0 (s, $C_{i'}$), 126.13 (d, ^1J(PC) = 50.56 Hz, C_α), 128.37 (d, ^3J(PC) = 10.81 Hz, C_m), 128.52 (d, ^3J(PC) = 10.56 Hz, C_m), 129.76 (s, $C_{o'}$), 129.83 (d, ^1J(PC) = 50.11 Hz, C_α), 130.24 (d, ^4J(PC) = 1.89 Hz, C_p), 130.79 (d, ^4J(PC) = 1.59 Hz, C_p), 131.39 (d, ^2J(PC) = 11.11 Hz, C_o), 132.01 (d, ^2J(PC) = 9.98 Hz, C_o), 132.42 (s, $C_{p'}$), 132.86 (d, ^1J(PC) = 45.35 Hz, C_i), 138.92 (s, C_5), 148.08 (s, C_6), 150.92 (d, ^2J(PC) = 9.75 Hz, C_β), 150.92 (d, ^2J(PC) = 10.66 Hz, C_β). The primed carbons are the S-C_6H_5 group. Anal. Calcd for $C_{37}H_{39}F_6OP_3RuS$: C, 52.92; H, 4.68. Found: C, 52.60; H, 5.23.

Intramolecular [4 + 2] Cycloaddition of [(η^5-C_5H_5)Ru(DMPP)$_2$(PhSCH=CH_2)]PF_6 (11). To a solution containing 1.00 g (1.37 mmol) of **1** in 50 mL of 1,2-dichloroethane was added 0.50 mL (3.02 mmol) of PhSCH=CH_2. The solution was heated at reflux for 12 h under N_2, the solvent was removed on a rotary evaporator, and the residue was washed with anhydrous diethyl ether, recrystallized from CH_2Cl_2/Et_2O, and vacuum-dried to afford 0.92 g (81.0%) of orange crystals: mp 160 °C dec. Anal. Calcd for $C_{37}H_{39}F_6P_3RuS$: C, 53.97; H, 4.74. Found: C, 54.00, 54.10; H, 4.60, 4.80.

Intramolecular [4 + 2] Cycloaddition of [(η^5-C_5H_5)Ru(DMPP)$_2$(2-vinylpyridine)]PF_6 (12). In an analogous manner **1** and 2-vinylpyridine produced an 80% yield of **12** after recrystallization from CH_2Cl_2/Et_2O/petroleum ether: mp 235–237 °C. ^1H NMR ($CDCl_3$): δ 1.47 (s, 3 H, 5-CH_3), 1.60 (s, 3 H, 6-CH_3), 1.75 (s, 3 H, β-CH_3), 2.00 (s, 3 H, β-CH_3), 2.08 (ddd, ^3J(PH) = 24.35, ^2J(H_3H_4) = 14.14, ^3J(H_2H_4) = 10.50 Hz, 1 H, H_4), 2.45 (apparent dt, ^2J(PH) = 3.00 Hz, ^3J(H_1H_2) = ^4J(H_1H_5) = 1.5 Hz, 1 H, H_1), 2.75 (apparent dq, ^2J(H_3H_4) = 14.14 Hz, ^3J(PH) = ^3J(H_3H_5) = ^3J(H_2H_3) = 1.50 Hz, 1 H, H_3), 3.19 (ddd, ^3J(PH) = 24.04, ^3J(H_2H_4) = 10.50, ^3J(H_2H_3) = 1.50 Hz, 1 H, H_2), 3.40 (apparent t, ^3J(H_3H_5) = ^4J(H_1H_5) = 1.50 Hz, 1 H, H_5), 4.83 (s,

Table II. Crystallographic Data for 4b, 5c, and 11

	4b	5c	11
chem formula	$C_{43}H_{44}F_6P_4Ru\cdot EtOH\cdot H_2O$	$C_{43}H_{44}F_6P_4Ru$	$C_{37}H_{39}F_6R_3Ru\cdot{}^1/_2CH_2Cl_2\cdot{}^1/_2H_2O$
fw	963.87	849.38	875.24
a, Å	20.965 (9)	11.137 (3)	11.392 (2)
b, Å	11.125 (4)	19.124 (5)	19.018 (5)
c, Å	21.678 (9)	8.686 (3)	35.610 (8)
β, deg	118.26 (2)	102.93 (2)	96.40 (2)
V, Å^3	4453.2	1803.1	7667.1
Z	4	2	8
space group	$P2_1/c$	$P2_1/m$	$C2/c$
T, °C	20	−100	20
λ, Å	0.710 73	1.5405	0.710 73
ρ(calcd), g cm^{-3}	1.438	1.564	1.429
μ, cm^{-1}	5.456	57.014	7.026
abs min/max	0.90/0.99	0.91/1.14	0.86/1.12
$R(F)^a$	0.051	0.042	0.048
$R_w(F)$	0.08	0.071	0.066

[a] Minimizing $\sum w(|F_o| - |F_c|)^2$ with $\sigma^2(F)^2 = \sigma^2(\text{counts}) + (pI)^2$.

5 H, C_5H_5), 6.07 (d, ^2J(PH) = 36.06 Hz, 1 H, H_α), 6.19 (d, ^2J(PH) = 35.76 Hz, 1 H, H_α), 6.49–8.60 (m, 14 H, Ph, Py). $^{13}C\{^1H\}$ NMR ($CDCl_3$): δ 14.17 (d, ^3J(PC) = 2.27 Hz, 5-CH_3), 14.35 (d, ^3J(PC) = 1.40 Hz, 6-CH_3), 16.85 (d, ^3J(PC) = 11.94 Hz, β-CH_3), 17.08 (d, ^3J(PC) = 11.41 Hz, β-CH_3), 33.19 (d, ^2J(PC) = 22.98 Hz, C_3), 46.77 (d, ^2J(PC) = 19.80 Hz, C_2), 47.91 (d, ^1J(PC) = 26.30 Hz, C_4), 54.84 (dd, ^1J(PC) = 29.40 Hz, ^3J(PC) = 3.0 Hz, C_1), 81.01 (t, ^2J(PC) = 1.66 Hz, C_5H_5), 121.72 (s, C_{II}), 127.86 (s, C_{III}), 127.98 (d, ^3J(PC) = 14.28 Hz, C_m), 128.03 (d, ^1J(PC) = 43.61 Hz, C_α), 128.10 (d, ^3J(PC) = 9.30 Hz, C_m), 128.65 (d, ^1J(PC) = 49.12 Hz, C_α), 129.29 (d, ^4J(PC) = 1.8 Hz, C_p), 129.52 (d, ^4J(PC) = 2.34 Hz, C_p), 130.0 (dd, ^1J(PC) = 45.10, ^3J(PC) = 2.70 Hz, C_i), 130.10 (d, ^2J(PC) = 8.99 Hz, C_o), 131.42 (d, ^2J(PC) = 11.94 Hz, C_o), 134.05 (s, C_5), 134.80 (dd, ^1J(PC) = 42.00, ^3J(PC) = 1.90 Hz, C_i), 137.15 (s, C_{IV}), 137.88 (s, C_6), 148.63 (d, ^2J(PC) = 8.54 Hz, C_β), 151.10 (d, ^2J(PC) = 8.46 Hz, C_β), 162.10 (d, ^3J(PC) = 1.51 Hz, C_I), 167.67 (s, C_V). Carbons with Roman numerals are pyridine ring carbons. Anal. Calcd for $C_{36}H_{38}F_6NP_3Ru$: C, 54.55; H, 4.83. Found: C, 54.37; H, 4.84.

[(η^5-C_5H_5)Ru(P∼P′)(Ph_3P)]Cl (13a,b). To a solution of dichloro[2-(vinylphenylphosphino)-5,6-dimethyl-7-phenyl-7-phosphabicyclo[2.2.1]-hept-5-ene]palladium(II)[3,4] (1.29 g, 2.45 mmol) in 100 mL of 1,2-dichloroethane was added 50 mL of a saturated aqueous sodium cyanide solution under N_2. The mixture was stirred with a magnetic stirring bar for 1 h to produce a colorless $ClCH_2CH_2Cl$ phase and a yellow-orange aqueous phase. The $ClCH_2CH_2Cl$ phase was separated filtered through Celite and anhydrous magnesium sulfate under nitrogen using Schlenk techniques, and added to 1.05 g (1.45 mmol) of (η^5-C_5H_5)Ru-(Ph_3P)$_2$Cl. The mixture was then heated at reflux under N_2 for 6 h. The solvent was removed on a rotary evaporator to give a mixture of **13a,b** in a 2:3 ratio, which was not further separated.

[(η^5-C_5H_5)Ru(DMPP)$_2$($Me_2NC(O)CH{=}CH_2$)]PF_6 (14). A solution containing 0.60 g (0.82 mmol) of **1** and 0.50 mL (4.86 mmol) of *N,N*-dimethylacrylamide in 20 mL of 1,2-dichloroethane was heated at reflux under nitrogen for 48 h. The solvent was removed on a rotary evaporator, and the resulting orange oil was washed with anhydrous diethyl ether (5 × 5 mL). The oil was crystallized from $CHCl_3$/petroleum ether (60–110 °C) to give a light yellow crystalline product, which was dried under vacuum: yield 0.24 g (37%); mp 192–196 °C dec. ^1H NMR ($CDCl_3$): δ 1.72 (s, 3 H, CH_3), 1.96 (s, 3 H, CH_3), 1.99 (s, 3 H, CH_3), 2.01 (s, 3 H, CH_3), 2.16 (dd, ^3J(PH) = 11.05, $^3J(H_aH_c)$ = 6.96 Hz, 1 H, H_c), 2.77 (apparent dt, ^3J(PH) = 14.23, $^3J(H_aH_c)$ = $^3J(H_aH_b)$ = 6.96 Hz, 1 H, H_a), 2.89 (s, 3 H, NCH_3), 2.97 (s, 3 H, NCH_3), 3.30 (apparent dt, $^3J(H_aH_b)$, = 6.96, ^3J(PH) = ^3J(PH) = 2.40 Hz, 1 H, H_b), 5.25 (s, 5 H, C_5H_5), 5.85 (d, ^2J(PH) = 33.46 Hz, 1 H, H_α), 6.32 (d, ^2J(PH) = 33.96 Hz, 1 H, H_α), 6.54 (d, ^2J(PH) = 33.06 Hz, 1 H, H_α), 6.59 (d, ^2J(PH) = 35.16 Hz, 1 H, H_α), 7.0–7.5 (m, 10 H, Ph). $^{13}C\{^1H\}$ NMR (DMSO-d_6): δ 16.29 (dd, ^3J(PC) = 10.66, ^5J(PC) = 1.59 Hz, β-CH_3), 16.63 (dd, ^3J(PC) = 10.69, ^5J(PC) = 1.89 Hz, β-CH_3), 16.90 (dd, ^3J(PC) = 11.37, ^5J(PC) = 1.47 Hz, β-CH_3), 17.24 (dd, ^3J(PC) = 10.12, ^5J(PC) = 1.13 Hz, β-CH_3), 35.64 (s, NCH_3), 36.69 (s, NCH_3), 45.45 (d, ^2J(PC) = 5.67 Hz, $=CH_2$), 46.85 (s, =CH), 87.55 (s, C_5H_5), 122.79 (d, ^2J(PC) = 45.35 Hz, C_α), 126.54 (d, ^2J(PC) = 41.19 Hz, C_α), 127.30 (d, ^2J(PC) = 48.37 Hz, C_α), 127.78 (d, ^2J(PC) = 47.62 Hz, C_α), 128.39 (d, ^3J(PC) = 9.37 Hz, C_m), 128.58 (d, ^3J(PC) = 9.90 Hz, C_m), 130.17 (s, C_p), 130.31 (s, C_p), 131.00 (d, ^1J(PC) = 40.74 Hz, C_i), 131.07 (d, ^2J(PC) = 9.22 Hz, C_o), 131.79 (d, ^2J(PC) = 8.69 Hz, C_o), 132.21 (d, ^1J(PC) = 40.74 Hz, C_i), 147.51 (d, ^2J(PC) = 8.01 Hz, C_β), 150.16 (d, ^2J(PC) = 8.99 Hz, C_β), 152.58 (d, ^2J(PC) = 8.99 Hz, C_β), 155.79 (d, ^2J(PC) = 9.50 Hz, C_β), 172.02 (s, >C=O). Anal. Calcd for $C_{34}H_{40}F_6NP_3Ru$: C, 51.93; H, 5.09; N, 1.78. Found: C, 51.96, 51.90; H, 5.10, 5.00; N, 1.60, 1.60.

[(η^5-C_5H_5)Ru(DMPP)$_2$($PhS(O)_2CH{=}CH_2$)]PF_6 (15). Similarly, from 0.50 g (0.68 mmol) of **1** and 0.23 g (1.36 mmol) of phenyl vinyl sulfone after crystallization from CH_2Cl_2/Et_2O at −14 °C and vacuum drying were obtained 0.30 g (51%) of yellow crystals: mp 146–149 °C dec. ^1H NMR ($CDCl_3$): δ 1.85 (s, 3 H, CH_3), 1.90 (ddd, ^3J(PH) = 17.10, $^3J(H_aH_c)$ = 7.60, $^3J(H_bH_c)$ = 2.90 Hz, 1 H, H_c), 1.99 (s, 3 H, CH_3), 2.07 (s, 3 H, CH_3), 2.14 (s, 3 H, CH_3), 3.13 (ddd, ^3J(PH) = 22.24, $^3J(H_aH_b)$ = 12.32, $^3J(H_aH_c)$ = 7.60 Hz, 1 H, H_a), 3.45 (apparent dt, $^3J(H_aH_b)$ = 12.32, $^3J(H_bH_c)$ = ^3J(PH) = 2.90 Hz, 1 H, H_b), 5.29 (s, 5 H, C_5H_5), 6.11 (d, ^2J(PH) = 34.56 Hz, 1 H, H_α), 6.38 (d, ^2J(PH) = 33.36 Hz, 1 H, H_α), 6.41 (d, ^2J(PH) = 35.76 Hz, 1 H, H_α), 7.05 (d, ^2J(PH) = 34.56 Hz, 1 H, H_α), 7.25–8.00 (m, 15 H, Ph). $^{13}C\{^1H\}$ NMR ($CDCl_3$): δ 17.09 (d, ^3J(PC) = 13.68 Hz, β-CH_3), 17.22 (d, ^3J(PC) = 13.08, β-CH_3), 17.49 (d, ^3J(PC) = 12.85 Hz, 2 β-CH_3), 30.65 (d, ^2J(PC) = 3.40 Hz, $=CH_2$), 68.83 (dd, ^2J(PC) = 6.50, ^2J(PC) = 1.81 Hz, =CH), 90.23 (s, C_5H_5), 124.30 (d, ^1J(PC) = 51.62 Hz, C_α), 125.28 (d, ^1J(PC) = 49.81 Hz, C_α), 127.01 (s, $C_{m'}$), 128.30 (d, ^1J(PC) = 50.79 Hz, C_α), 128.49 (d, ^3J(PC) = 10.20 Hz, C_m), 128.54 (d, ^1J(PC) = 49.80 Hz, C_i), 129.26 (d, ^3J(PC) = 10.28 Hz, C_m), 129.53 (s, $C_{o'}$), 129.50 (d, ^1J(PC) = 50.79 Hz, C_i), 130.78 (d, ^4J(PC) = 2.72 Hz, C_p), 130.95 (d, ^4J(PC) = 2.72 Hz, C_p), 131.13 (d, ^2J(PC) = 9.15 Hz, C_o), 132.48 (d, ^2J(PC) = 8.84 Hz, C_o), 132.50 (dd, ^1J(PC) = 51.54, ^3J(PC) = 2.90 Hz, C_i), 133.30 (s, $C_{p'}$), 142.68 (s, $C_{i'}$), 150.60 (d, ^2J(PC) = 9.83 Hz, C_β), 151.62 (d, ^2J(PC) = 9.90 Hz, C_β), 152.52 (d, ^2J(PC) = 10.20 Hz, C_β), 153.92 (d, ^2J(PC) = 8.69 Hz, C_β). The primed carbons are the SO_2Ph group. Anal. Calcd for $C_{37}H_{39}F_6O_2P_3RuS$: C, 51.93; H, 4.59. Found: C, 51.58; H, 4.67.

[(η^5-C_5H_5)Ru(DMPP)$_2$(L)]PF_6: L = $P(OCH_2CH{=}CH_2)_3$ (16), $P(C{\equiv}CPh)_3$ (17), $H_2NCH_2CH{=}CH_2$ (18), $N{\equiv}C{-}CH{=}CH_2$ (19), $N(CH_2C(CH_3){=}CH_2)_3$ (20), and $C_2H_5OCH{=}CH_2$ (21). All these complexes were similarly prepared from **1** and the appropriate L in high yield. They were only characterized by $^{31}P\{^1H\}$ NMR spectroscopy.

C. X-ray Data Collection and Processing. Crystals of **4b** (yellow), **5c** (colorless), and **11** (orange) were isolated from CH_2Cl_2/C_2H_5OH (95%), acetone/CH_2Cl_2, and $CH_2Cl_2/CHCl_3$/petroleum ether solutions, respectively, at room temperature. Crystal data and details of data collection are given in Table II. For both **4b** and **11**, single crystals were cut out from a cluster of crystals and mounted on a rotation-free goniometer head. Systematic searches in reciprocal space with a Philips PW 100/16 automatic diffractometer for **5c** and a CAD-4 diffractometer for **4b** and **11** showed that crystals of all three complexes belong to the monoclinic system.

Table III. Atom Coordinates for 5c[a]

atom	x	y	z	B, Å²
Ru	0.33455 (4)	0.250	0.23613 (5)	1.91 (1)
P1	0.2317 (1)	1.16216 (6)	0.3207 (1)	2.22 (2)
C1	0.2369 (4)	0.1611 (2)	0.5369 (5)	2.25 (9)
C2	0.1980 (4)	0.0862 (2)	0.5619 (5)	2.5 (1)
C3	0.2406 (4)	0.0416 (2)	0.4696 (5)	2.6 (1)
C4	0.3217 (4)	0.0795 (2)	0.3759 (5)	2.7 (1)
C5	0.1252 (4)	0.0718 (3)	0.6828 (6)	3.3 (1)
C6	0.2311 (4)	−0.0362 (3)	0.4657 (6)	3.6 (1)
C7	0.3796 (4)	0.1686 (2)	0.5880 (5)	2.4 (1)
C8	0.4326 (4)	0.1083 (2)	0.5017 (6)	2.6 (1)
C9	0.0779 (4)	0.1375 (3)	0.2165 (5)	2.7 (1)
C10	0.0596 (5)	0.1049 (4)	0.0756 (7)	7.4 (2)
C11	−0.0577 (6)	0.0866 (5)	−0.0047 (8)	9.7 (2)
C12	−0.1570 (5)	0.1030 (3)	0.0468 (7)	5.3 (1)
C13	−0.1420 (5)	0.1363 (3)	0.1843 (8)	5.4 (2)
C14	−0.0228 (5)	0.1533 (3)	0.2693 (7)	4.7 (1)
P2	0.4282 (1)	0.250	0.4983 (2)	2.14 (3)
C15	0.5948 (6)	0.250	0.5780 (8)	2.7 (1)
C16	0.6404 (6)	0.250	0.7413 (9)	4.3 (2)
C17	0.7663 (7)	0.250	0.805 (1)	5.1 (2)
C18	0.8470 (6)	0.250	0.708 (1)	5.1 (2)
C19	0.8025 (6)	0.250	0.547 (1)	5.8 (2)
C20	0.6747 (6)	0.250	0.4782 (9)	4.1 (2)
C21	0.2801 (6)	0.250	−0.0257 (8)	2.9 (2)
C22	0.3527 (4)	0.3100 (2)	0.0196 (5)	2.6 (1)
C23	0.4721 (4)	0.2873 (2)	0.0969 (5)	2.9 (1)
P3	0.500	0.500	0.000	2.51 (4)
F1	0.3616 (2)	0.4771 (2)	−0.0002 (4)	4.44 (7)
F2	0.4518 (3)	0.5450 (2)	−0.1543 (3)	4.45 (7)
F3	0.5155 (3)	0.4331 (2)	−0.1021 (4)	4.38 (7)

[a] Anisotropically refined atoms are given in the form of the isotropic equivalent displacement parameter defined as $^4/_3[a^2\beta_{11} + b^2\beta_{22} + c^2\beta_{33} + ab(\cos\gamma)\beta_{12} + ac(\cos\beta)\beta_{13} + bc(\cos\alpha)\beta_{23}]$.

It was found that **11** crystallized with $^1/_2$ CH_2Cl_2 and $^1/_2$ H_2O per complex. Half of the PF_6 anion lies on an inversion center and the other half on a C_2 axis with two F atoms on the axis. The carbon atom of CH_2Cl_2 and the oxygen atom of H_2O also lie on the C_2 axis. Complex **4b** crystallized with 1 C_2H_5OH and 1 H_2O molecule per complex.

Quantitative data were obtained at −100 °C, achieved with a locally built gas flow device, for **5c**. For **4b** and **11** data were obtained at room temperature. The resulting data sets were transferred to a VAX computer, and for all subsequent calculations the Enraf-Nonius SDP/VAX package[22] was used with the exception of a local data reduction program. Three standard reflections measured every 1 h during the entire data collection periods showed no significant trends. The raw step-scan data for **5c** were converted to intensities by using the Lehmann–Larsen method[23] and then corrected for Lorentz and polarization factors. The raw data for **4b** and **11** were similarly converted to intensities and corrected for Lorentz, polarization, and absorption factors, the last being based on ψ scans. The centrosymmetric space group $P2_1/m$ was assumed for **5c** on the basis of an N_Z cumulative test. The structures were solved by using the heavy-atom method. For **5c** both molecular fragments lie in special positions of the space group: the cationic moiety lies on a plane through Ru, P2, the six phenyl carbons C_{15}–C_{20}, and C_{21} of the cyclopentadienyl ring; the PF_6 anion lies on an inversion center. After refinement of the heavy atoms, difference Fourier maps revealed maxima of residual electronic density close to the positions expected for the hydrogen atoms. They were introduced in the structure factor calculations by their computed coordinates (CH = 0.95 Å) with isotropic temperature factors such as $B(H) = 1.3[B_{eqv}(C)]$ Å² but were not refined. For **11** the H_2O and CH_2Cl_2 and for **4b** the C_2H_5OH and H_2O hydrogen atoms were omitted. At this stage empirical absorption corrections were applied for **5c** using the method of Walker and Stuart,[24] since face indexation was not possible under the cold gas stream. Full least-squares refinements minimizing $\sum w(|F_o| - |F_c|)^2$ with $\sigma^2(F)^2 = \sigma^2_{counts} + (pI)^2$ converged to the values given in Table II. Final difference maps revealed no significant maxima. The scattering factors coefficients and anomalous dispersion coefficients come respectively from parts a and b of ref 25. Final atom coordinates for **5c**, **11**, and **4b** are given in Tables III, VI, and IX and selected bond lengths and angles in Tables IV, V, VII, VIII, X, and XI, respectively.

Results

Ligand substitution[26] of CH_3CN in $[(\eta^5\text{-}C_5H_5)Ru(CH_3CN)_3]PF_6$ to produce $[(\eta^5\text{-}C_5H_5)RuL_2(CH_3CN)]PF_6$ (L = DMPP (**1**), DPVP (**2**), DVPP (**3**)) is a facile process. Complex **1** reacts with a variety of dieneophilic ligands L′ to form $[(\eta^5\text{-}C_5H_5)Ru(DMPP)_2L']PF_6$ complexes that undergo spontaneous intramolecular [4 + 2] Diels–Alder cycloadditions, as illustrated in reactions 9–15.

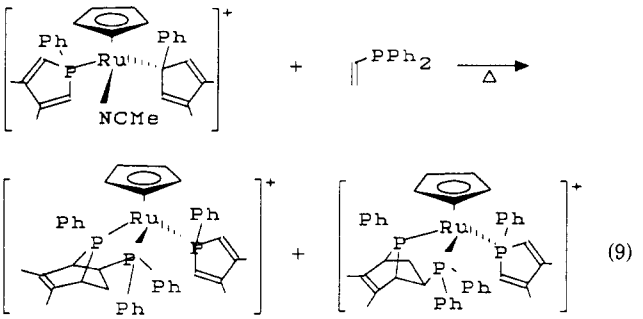

(9)

4a:4b::5:1

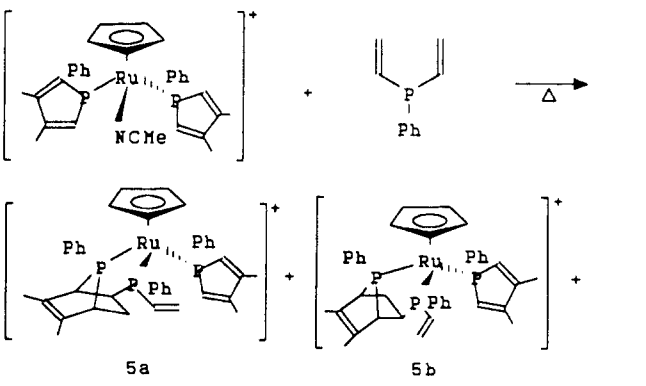

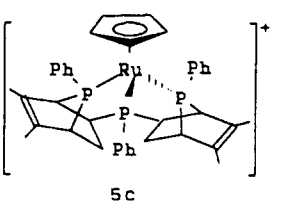

(10)

5a:5b:5c::3:1:4

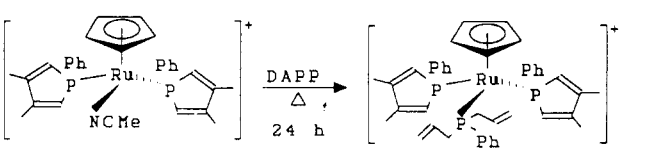

(11)

(22) Frenz, B. A. In *Computing in Crystallography*; Schenk, H. Olthof-Hazekamp, R., Van Koningsveld, H., Bassi, G. C., Eds.; Delft University Press: Delft, The Netherlands, 1978; pp 64–71.

(23) Lehmann, M. S.; Larsen, F. K. *Acta Crystallogr., Sect. A: Cryst. Phys., Diffr., Theor. Gen. Crystallogr.* **1974**, *A30*, 580.

(24) Walker, N.; Stuart, D. *Acta Crystallogr., Sect. A: Struct. Crystallogr. Cryst. Chem.* **1983**, *A39*, 158.

(25) (a) Cromer, D. T.; Waber, J. T. *International Tables for X-ray Crystallography*; Kynoch: Birmingham, England, 1974; Table 2.2B. (b) *Ibid.*, Table 2.3.1.

(26) Luginbühl, W.; Zbinden, P.; Pittet, P. A.; Armbruster, T.; Burgi, H.; Merbach, A. E.; Ludi, A. *Inorg. Chem.* **1991**, *30*, 2350.

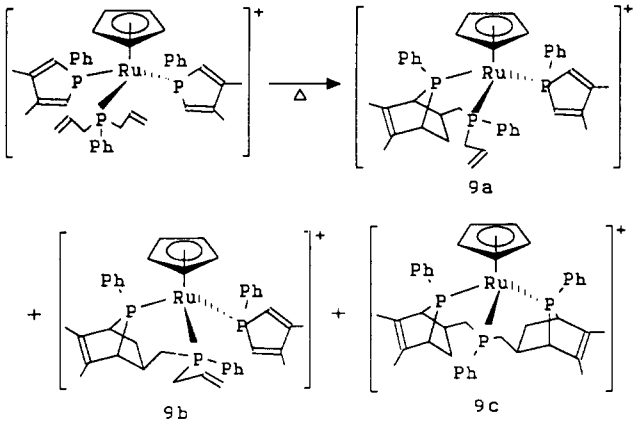

9a:9b:9c::3:1:1

(12)

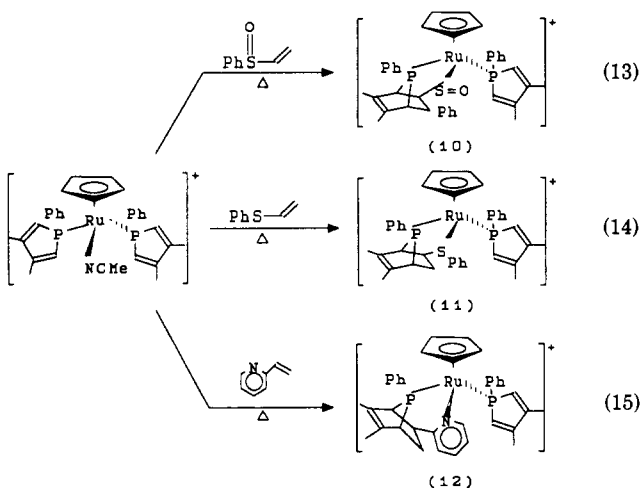

(13)

(14)

(15)

Similarly, **2** and **3** react with DMPP as shown in reactions 16 and 17.

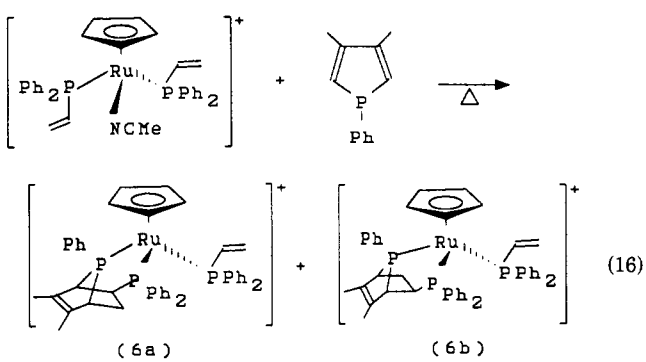

6a:6b:9:1

(16)

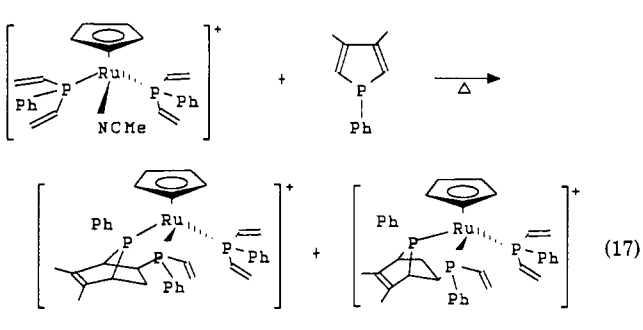

7a:7b::6:1

(17)

These reactions provide ready syntheses of chiral complexes containing a variety of conformationally rigid chiral bidentate or tridentate ligands with diastereoselectivities that are a function of the magnitudes of interligand steric effects. New compounds were characterized by ^1H, $^{13}C\{^1H\}$, and $^{31}P\{^1H\}$ NMR spectroscopy. Assignments were made by previously described techniques[2-8] and are given in the Experimental Section with atom-numbering schemes similar to those used previously.[2-8] These spectra are characteristic of the assigned structures.

In contrast to these reactions, **1** reacted with $Me_2NC(O)CH{=}CH_2$, $PhS(O)_2CH{=}CH_2$, $P(OCH_2CH{=}CH_2)_3$, $P(C{\equiv}CPh)_3$, $H_2NCH_2CH{=}CH_2$, $N{\equiv}C{-}CH{=}CH_2$, $N(CH_2C(CH_3){=}CH_2)_3$, and $C_2H_5OCH{=}CH_2$ to form only the ligand substitution products **14–21**, none of which could be induced to undergo Diels–Alder cycloadditions. The vinyl groups of $Me_2NC(O)CH{=}CH_2$ and $PhS(O)_2CH{=}CH_2$ are coordinated to ruthenium in **14** and **15**.

Table IV. Selected Bond Distances (Å) for Complex 5c[a]

Ru–P1	2.247 (1)	C2–C3	1.328 (6)
Ru–P1′	2.247 (1)	C2–C5	1.448 (6)
Ru–P2	2.283 (2)	C3–C4	1.528 (6)
Ru–C21	2.218 (6)	C3–C6	1.491 (7)
Ru–C22	2.251 (4)	C4–C8	1.555 (6)
Ru–C23	2.269 (5)	C7–C8	1.561 (6)
P1–C1	1.866 (4)	C7–P2	1.875 (4)
P1–C4	1.875 (4)	P2–C15	1.829 (6)
P1–C9	1.812 (4)	C21–C22	1.408 (6)
C1–C2	1.527 (6)	C22–C23	1.417 (6)
C1–C7	1.558 (6)	C23–C23′	1.427 (9)

[a] Numbers in parentheses are estimated standard deviations in the least significant digits.

Table V. Selected Bond Angles (deg) for Complex 5c[a]

P1–Ru–P1′	96.77 (6)	C22′–Ru–C23	61.1 (2)
P1–Ru–P2	80.00 (4)	C22′–Ru–C23′	36.5 (2)
P1–Ru–C21	107.0 (1)	C23–Ru–C23′	36.6 (2)
P1–Ru–C22	143.3 (1)	C1–P1–C4	80.7 (2)
P1–Ru–C22′	92.3 (1)	C1–P1–C9	108.2 (2)
P1–Ru–C23	149.7 (1)	C4–P1–C9	107.4 (2)
P1′–Ru–C23	113.2 (1)	P1–C1–C2	102.0 (3)
P1′–Ru–P2	80.00 (4)	P1–C1–C7	94.9 (3)
P1–Ru–C21	107.0 (1)	C2–C1–C7	110.5 (3)
P1–Ru–C22′	92.3 (1)	C1–C2–C3	111.4 (4)
P1–Ru–C22	143.3 (1)	C1–C2–C5	119.4 (4)
P1–Ru–C23	113.2 (1)	C3–C2–C5	129.2 (4)
P1–Ru–C23′	149.7 (1)	C2–C3–C4	110.5 (4)
P2–Ru–C21	169.0 (2)	C2–C3–C6	128.4 (4)
P2–Ru–C22	136.7 (1)	C4–C3–C6	120.6 (4)
P2–Ru–C22′	136.7 (1)	P1–C4–C3	101.0 (3)
P2–Ru–C23	108.6 (1)	P1–C4–C8	100.2 (3)
P2–Ru–C23′	108.6 (1)	C3–C4–C8	105.4 (3)
C21–Ru–C22	36.7 (1)	C1–C7–C8	105.5 (3)
C21–Ru–C22′	36.7 (1)	C1–C7–P2	109.2 (3)
C21–Ru–C23	61.0 (2)	C8–C7–P2	103.8 (3)
C21–Ru–C23′	61.0 (2)	C4–C8–C7	105.8 (3)
C22–Ru–C22′	61.3 (2)	C7–P2–C7′	112.3 (3)
C22–Ru–C23	36.5 (2)	C7–P2–C15	101.9 (2)
C22–Ru–C23′	61.1 (2)	C7′–P2–C15′	101.9 (2)

[a] Numbers in parentheses are estimated standard deviations in the least significant digits.

Discussion

Although half-sandwich ruthenium complexes have been widely studied,[27] only a limited number of complexes of the $[(\eta^5\text{-}C_5H_5)Ru(P{\sim}P)X]^{n+}$ type (P∼P is a bidentate diphosphine; X is an anionic (n = 0) or neutral (n = 1) ligand) have been synthesized. Previous syntheses have usually involved reaction of $[(\eta^5\text{-}C_5H_5)Ru(PPh_3)_2X]^{n+}$ or $[(\eta^5\text{-}C_5H_5)Ru(CO)_2X]^{n+}$ with a chiral diphosphine.[28] The

(27) Szczepura, L. F.; Takeuchi, K. J. *Inorg. Chem.* **1990**, *29*, 1772 and references therein.

Table VI. Atom Coordinates for 11[a]

atom	x	y	z	B, Å²
Ru	0.29415 (5)	0.27591 (4)	0.60282 (2)	2.70 (1)
S	−0.1807 (2)	0.8090 (1)	0.66699 (6)	3.04 (4)
P1	−0.2992 (2)	0.8821 (1)	0.59883 (6)	2.84 (4)
P2	0.1258 (2)	0.2173 (1)	0.61297 (6)	2.88 (4)
C1	−0.3231 (7)	0.9173 (4)	0.6455 (2)	2.9 (2)
C2	−0.3389 (7)	0.9946 (5)	0.6385 (2)	3.4 (2)
C3	−0.2721 (7)	1.0173 (5)	0.6126 (3)	3.8 (2)
C4	−0.1971 (8)	0.9581 (5)	0.6015 (3)	3.9 (2)
C5	−0.4188 (9)	1.0368 (5)	0.6606 (3)	4.9 (2)
C6	−0.255 (1)	1.0910 (6)	0.5986 (3)	5.7 (3)
C7	−0.1149 (7)	0.9378 (5)	0.6374 (3)	3.8 (2)
C8	−0.1946 (7)	0.9056 (4)	0.6638 (3)	3.4 (2)
C9	−0.4255 (7)	0.9029 (4)	0.5658 (3)	3.5 (2)
C10	−0.5314 (7)	0.9285 (5)	0.5761 (3)	4.3 (2)
C11	−0.6271 (8)	0.9424 (6)	0.5495 (3)	5.1 (2)
C12	−0.6214 (9)	0.9297 (6)	0.5124 (3)	5.8 (3)
C13	−0.517 (1)	0.9016 (7)	0.5015 (3)	7.4 (3)
C14	−0.4195 (9)	0.8882 (6)	0.5280 (3)	5.6 (3)
C15	−0.0315 (7)	0.7959 (5)	0.6886 (2)	3.5 (2)
C16	0.0410 (8)	0.8486 (5)	0.7025 (3)	4.7 (2)
C17	0.1497 (8)	0.8329 (6)	0.7206 (3)	5.3 (3)
C18	0.1858 (8)	0.7650 (7)	0.7263 (3)	5.9 (3)
C19	0.113 (1)	0.7123 (7)	0.7131 (3)	6.5 (3)
C20	0.0036 (8)	0.7268 (6)	0.6943 (3)	4.9 (2)
C21	0.0184 (7)	0.2562 (5)	0.6408 (3)	3.4 (2)
C22	−0.0843 (7)	0.2643 (4)	0.6188 (3)	3.8 (2)
C23	−0.0851 (8)	0.2383 (5)	0.5798 (3)	3.9 (2)
C24	0.0167 (8)	0.2079 (4)	0.5728 (2)	3.6 (2)
C25	−0.1914 (8)	0.2976 (6)	0.6321 (4)	6.0 (3)
C26	−0.1928 (9)	0.2455 (6)	0.5515 (4)	6.6 (3)
C27	0.1562 (7)	0.1299 (5)	0.6318 (3)	3.6 (2)
C28	0.1335 (8)	0.0710 (5)	0.6103 (3)	4.2 (2)
C29	0.1688 (9)	0.0052 (5)	0.6241 (3)	5.4 (3)
C30	0.2256 (9)	−0.0017 (5)	0.6600 (3)	5.9 (3)
C31	0.249 (1)	0.0568 (6)	0.6821 (3)	6.3 (3)
C32	0.2136 (8)	0.1229 (5)	0.6682 (3)	4.5 (2)
C33	0.152 (1)	0.2331 (7)	0.4540 (3)	7.4 (3)
C34	0.1725 (9)	0.2974 (6)	0.4422 (3)	6.7 (3)
C35	0.096 (1)	0.3135 (6)	0.4120 (3)	7.0 (3)
C36	0.0237 (8)	0.2584 (8)	0.4039 (3)	7.7 (3)
C37	0.056 (1)	0.2048 (6)	0.4300 (3)	7.7 (3)
P3	0.000	0.000	0.500	4.85 (9)
F1	−0.0747 (6)	0.0494 (4)	0.5242 (2)	8.7 (2)
F2	−0.0502 (7)	0.0403 (4)	0.4628 (2)	8.6 (2)
F3	−0.1090 (6)	−0.0509 (4)	0.4930 (2)	8.7 (2)
P4	0.00	0.4062 (2)	0.750	5.00 (9)
F4	0.1193 (7)	0.4128 (7)	0.7336 (2)	15.4 (4)
F5	0.4385 (6)	−0.0935 (5)	0.7078 (2)	8.7 (2)
F6	0.000	0.4895 (7)	0.750	12.5 (5)
F7	0.000	0.3284 (7)	0.750	20.5 (8)
OW	0.000	0.1772 (4)	0.750	5.4 (2)
C38	0.000	0.0152 (8)	0.750	9.9 (6)
Cl	0.112 (1)	0.0571 (5)	0.7741 (3)	17.9 (3)

[a] See footnote *a* in Table III.

Table VII. Selected Bond Distances (Å) for Complex 11[a]

Ru-S	2.357 (2)	C1-C8	1.55 (1)
Ru-P1	2.280 (2)	C2-C3	1.33 (1)
Ru-P2	2.281 (2)	C2-C5	1.50 (1)
Ru-C33	2.187 (9)	C3-C4	1.49 (1)
Ru-C34	2.19 (1)	C3-C6	1.51 (1)
Ru-C35	2.21 (1)	C4-C7	1.55 (1)
Ru-C36	2.213 (9)	C7-C8	1.51 (1)
Ru-C37	2.219 (1)	C21-C22	1.34 (1)
S-C8	1.803 (8)	C22-C23	1.48 (1)
S-C15	1.803 (8)	C22-C25	1.50 (1)
P1-C1	1.840 (7)	C23-C24	1.34 (1)
P1-C4	1.850 (8)	C23-C26	1.50 (1)
P1-C9	1.796 (8)	C33-C34	1.32 (2)
P2-C21	1.816 (8)	C33-C37	1.41 (2)
P2-C24	1.796 (8)	C34-C35	1.34 (2)
P2-C27	1.809 (8)	C35-C36	1.34 (2)
C1-C2	1.50 (1)	C36-C37	1.40 (2)

[a] Numbers in parentheses are estimated standard deviations in the least significant digits.

Table VIII. Selected Bond Angles (deg) for Complex 11[a]

S-Ru-P1	80.16 (7)	C1-C2-C5	120.5 (7)
S-Ru-P2	89.45 (7)	C3-C2-C5	128.1 (8)
S-Ru-C33	154.4 (5)	C2-C3-C4	109.2 (7)
S-Ru-C34	150.2 (5)	C2-C3-C6	129.4 (8)
S-Ru-C35	115.2 (4)	C4-C3-C6	120.9 (7)
S-Ru-C36	99.7 (3)	P1-C4-C3	103.1 (5)
S-Ru-C37	116.9 (5)	P1-C4-C7	99.6 (5)
P1-Ru-P2	92.78 (7)	C3-C4-C7	106.2 (7)
P1-Ru-C33	100.9 (3)	C4-C7-C8	105.4 (6)
P1-Ru-C34	129.5 (5)	S-C8-C1	103.8 (5)
P1-Ru-C35	160.0 (3)	S-C8-C7	112.9 (5)
P1-Ru-C36	133.7 (6)	C1-C8-C7	106.6 (7)
P1-Ru-C37	101.8 (4)	P1-C9-C10	124.1 (7)
P2-Ru-C33	115.9 (5)	P1-C9-C14	118.0 (6)
P2-Ru-C34	91.3 (3)	S-C15-C16	124.1 (7)
P2-Ru-C35	99.8 (4)	S-C15-C20	116.0 (6)
P2-Ru-C36	133.4 (6)	P2-C21-C22	109.0 (6)
P2-Ru-C37	151.6 (4)	C21-C22-C23	115.1 (1)
C8-S-C15	103.5 (4)	C21-C22-C25	123.6 (9)
C1-P1-C4	79.9 (4)	C23-C22-C25	121.3 (8)
C1-P1-C9	108.8 (4)	C22-C23-C24	113.8 (7)
C4-P1-C9	108.4 (4)	P2-C27-C28	122.0 (7)
C21-P2-C24	91.5 (4)	P2-C27-C32	118.9 (7)
C21-P2-C27	106.5 (4)	P2-C24-C23	110.2 (6)
C24-P2-C27	106.9 (4)	C2-C1-C8	107.6 (6)
P1-C1-C2	103.5 (5)	C1-C2-C3	111.4 (7)
P1-C1-C8	95.8 (5)	C34-C33-C37	108.0 (1)

[a] Numbers in parentheses are estimated standard deviations in the least significant figures.

diastereoselectivity in these reactions is generally low,[28,29] epimerization often occurs,[28,29] and prior syntheses of the ligands are required. These two approaches were generally unsuccessful with monodentate ligands, except for phosphites. Ligands such as DMPP, $Ph_2PCH{=}CH_2$, or $PhP(CH{=}CH_2)_2$ did not replace PPh_3 or CO even at elevated temperatures and/or with prolonged reaction times. However, Gill and Mann's[17] synthesis of $[(\eta^5\text{-}C_5H_5)Ru(CH_3CN)_3]PF_6$ opened a new era for the preparation of complexes of the type $[(\eta^5\text{-}C_5H_5)RuLL'L'']PF_6$. They reported that one, two, or three acetonitrile ligands could be selectively replaced, depending upon reaction conditions, although their reported examples only involved phosphite ligands. With DMPP, DVPP, or DPVP, however, we find that, even with 1:1 ligand to metal ratios, mixtures of the mono- and disubstitution products are quickly formed in acetonitrile solution at ambient temperature. Pure $[(\eta^5\text{-}C_5H_5)RuL_2(CH_3CN)]PF_6$ complexes were easily prepared by overnight reactions at room temperature with 2:1 ligand to metal ratios.

We have previously shown that [4 + 2] cycloadditions of vinylphosphines with DMPP within the coordination spheres of Mo(0),[8] Ni(II),[2] Pd(II),[3,4] Pt(II),[3,4] or Ru(II)[6,7] complexes occur readily. Except for some for the platinum reactions,[5] the mixed-ligand phosphole–vinylphosphine intermediates were not observed in these reactions. Similarly, except for reaction 11, no mixed-ligand intermediates were observed. Diels–Alder products were formed immediately upon ligand substitution.

On the basis of previous studies, when both substituents on the exocyclic phosphorus are the same, only one pair of diastereomers of the diphosphine [4 + 2] cycloadducts

(28) (a) Consiglio, G.; Morandini, F. *Chem. Rev.* **1987**, *87*, 761. (b) Morandini, F.; Consiglio, G.; Straub, B.; Ciani, G.; Sironi, A. *J. Chem. Soc., Dalton Trans* **1983**, 2293. (c) Ashby, G. S.; Bruce, M. I.; Tomkins, I. B.; Wallis, R. C. *Aust. J. Chem.* **1979**, *32*, 1003. (d) Fryzuk, M. D.; Bosnich, B. *J. Am. Chem. Soc.* **1978**, *100*, 5491. (e) *J. Am. Chem. Soc.* **1977**, *99*, 6262. (f) Riley, D. P.; Shumate, R. *J. Org. Chem.* **1980**, *45*, 5187. (g) King, R. B.; Bakos, J.; Hoff, C. C.; Markó, L. *J. Org. Chem.* **1979**, *44*, 1729.

(29) Consiglio, G.; Morandini, F.; Bangerter, F. *Inorg. Chem.* **1979**, *44*, 1729.

Table IX. Atom Coordinates for 4b[a]

atom	*x*	*y*	*z*	*B*, Å^2
Ru	0.21808 (2)	0.03964 (5)	0.37332 (2)	2.437 (9)
P1	0.34235 (7)	0.0474 (2)	0.44173 (7)	2.43 (3)
C1	0.3844 (3)	0.1018 (6)	0.5319 (3)	2.6 (1)
C2	0.4463 (3)	0.0500 (7)	0.5844 (3)	3.7 (2)
C3	0.4807 (4)	0.1018 (8)	0.6506 (3)	4.7 (2)
C4	0.4527 (4)	0.2062 (8)	0.6628 (4)	5.4 (2)
C5	0.3912 (4)	0.2566 (7)	0.6115 (4)	4.8 (2)
C6	0.3560 (3)	0.2041 (6)	0.5457 (3)	3.5 (2)
C7	0.3894 (3)	0.1407 (6)	0.4053 (3)	2.7 (1)
C8	0.4358 (3)	0.2343 (6)	0.4441 (3)	3.3 (1)
C9	0.4675 (3)	0.3064 (6)	0.4136 (3)	3.8 (2)
C10	0.4554 (3)	0.2864 (7)	0.3474 (3)	4.4 (2)
C11	0.4112 (4)	0.1929 (7)	0.3096 (3)	4.4 (2)
C12	0.3773 (3)	0.1227 (6)	0.3370 (3)	3.5 (2)
C13	0.3780 (3)	−0.1067 (6)	0.4482 (3)	2.7 (1)
C14	0.3525 (3)	−0.1805 (6)	0.4940 (3)	2.7 (1)
C15	0.2872 (3)	−0.2571 (6)	0.4421 (3)	2.9 (1)
C16	0.3203 (3)	−0.3538 (6)	0.4165 (3)	3.2 (1)
C17	0.3519 (3)	−0.3029 (6)	0.3819 (3)	3.0 (1)
C18	0.3388 (3)	−0.1684 (6)	0.3746 (3)	2.7 (1)
C19	0.3205 (4)	−0.4826 (6)	0.4356 (4)	5.0 (2)
C20	0.3976 (4)	−0.3623 (7)	0.3539 (3)	4.5 (2)
P2	0.24665 (8)	−0.1549 (2)	0.36526 (7)	2.62 (3)
C21	0.1867 (3)	−0.2470 (6)	0.2907 (3)	3.2 (1)
C22	0.1459 (4)	−0.3386 (8)	0.2984 (4)	4.8 (2)
C23	0.1003 (5)	−0.4068 (9)	0.2406 (5)	6.7 (3)
C24	0.0951 (5)	−0.3856 (9)	0.1761 (4)	7.1 (3)
C25	0.1358 (5)	−0.296 (1)	0.1694 (4)	6.7 (3)
C26	0.1801 (4)	−0.2260 (8)	0.2253 (3)	4.9 (2)
P3	0.81470 (8)	0.9954 (2)	0.54010 (8)	2.61 (3)
C27	0.9000 (3)	1.0808 (6)	0.5690 (3)	3.3 (2)
C28	0.9298 (3)	1.0934 (7)	0.5246 (3)	4.1 (2)
C29	0.9927 (4)	1.1585 (8)	0.5448 (4)	5.4 (2)
C30	1.0252 (4)	1.2122 (8)	0.6090 (4)	5.9 (2)
C31	0.9959 (4)	1.1993 (8)	0.6535 (4)	5.6 (2)
C32	0.9341 (3)	1.1340 (7)	0.6344 (3)	4.0 (2)
C33	0.7598 (3)	1.0573 (6)	0.4544 (3)	3.3 (1)
C34	0.7517 (3)	0.9778 (7)	0.4043 (3)	3.5 (1)
C35	0.7908 (3)	0.8650 (7)	0.4318 (3)	3.6 (1)
C36	0.8287 (3)	0.8608 (6)	0.5020 (3)	3.4 (1)
C37	0.7065 (5)	1.0016 (9)	0.3277 (4)	6.1 (3)
C38	0.7865 (4)	0.7667 (8)	0.3833 (4)	6.0 (2)
C39	0.1244 (4)	0.0624 (7)	0.2675 (4)	4.9 (2)
C40	0.1879 (4)	0.1038 (7)	0.2659 (3)	4.8 (2)
C41	0.2133 (4)	0.2032 (7)	0.3107 (3)	4.3 (2)
C42	0.1675 (4)	0.2234 (7)	0.3404 (4)	4.4 (2)
C43	0.1121 (4)	0.1341 (7)	0.3135 (4)	4.4 (2)
P4	0.6791 (1)	0.0960 (2)	0.8516 (1)	6.02 (6)
F1	0.7078 (4)	0.0160 (8)	0.9192 (3)	13.1 (3)
F2	0.6062 (3)	0.0222 (6)	0.8146 (3)	9.4 (2)
F3	0.6554 (4)	0.1665 (6)	0.7822 (3)	11.0 (2)
F4	0.7507 (3)	0.1723 (6)	0.8865 (3)	9.6 (2)
F5	0.7175 (5)	0.0041 (6)	0.8259 (4)	13.6 (3)
F6	0.6456 (3)	0.1828 (8)	0.8805 (3)	16.2 (2)
C44	0.0335 (8)	0.109 (2)	0.8754 (8)	14.1 (5)*
C45	0.0780 (5)	0.0329 (9)	0.9025 (5)	6.5 (2)*
O	0.1249 (7)	0.985 (1)	0.9616 (6)	19.0 (5)
OW	0.9153 (5)	0.009 (1)	0.9620 (5)	17.6 (4)

[a] See footnote *a* in Table III.

Table X. Selected Bond Distances (Å) for Complex 4b[a]

Ru–P1	2.310 (1)	C17–C18	1.515 (8)
Ru–P2	2.274 (2)	C17–C20	1.510 (8)
Ru–P3	2.317 (2)	C18–P2	1.850 (6)
Ru–C39	2.218 (6)	P2–C21	1.822 (6)
Ru–C40	2.222 (6)	P3–C27	1.852 (6)
Ru–C41	2.244 (6)	P3–C33	1.797 (6)
Ru–C42	2.257 (7)	P3–C36	1.800 (6)
Ru–C43	2.234 (6)	C33–C34	1.346 (8)
P1–C1	1.825 (5)	C34–C35	1.463 (9)
P1–C7	1.847 (6)	C34–C37	1.495 (9)
P1–C13	1.848 (6)	C35–C36	1.343 (8)
C13–C14	1.564 (7)	C35–C38	1.489 (9)
C13–C18	1.566 (7)	C39–C40	1.42 (1)
C14–C15	1.550 (8)	C39–C43	1.39 (1)
C15–C16	1.519 (8)	C40–C41	1.40 (1)
C15–P2	1.857 (6)	C42–C43	1.43 (1)
C16–C17	1.340 (8)	C41–C42	1.406 (9)
C16–C19	1.492 (8)	C31–C32	1.367 (9)

[a] Numbers in parentheses are estimated standard deviations in the least significant figures.

Table XI. Selected Bond Angles (deg) for Complex 4b[a]

P1–Ru–P2	80.02 (5)	C17–C18–P2	102.7 (4)
P1–Ru–P2	99.40 (5)	C15–P2–C18	80.9 (3)
P2–Ru–P3	95.28 (5)	C15–P2–C21	106.4 (3)
C1–P1–C7	100.8 (3)	C18–P2–C21	107.3 (3)
C1–P1–C13	104.6 (3)	C27–P3–C33	101.3 (3)
C7–P1–C13	106.0 (2)	C27–P3–C36	103.9 (3)
P1–C13–C14	106.7 (4)	C33–C3–C36	90.4 (3)
P1–C13–C18	109.3 (4)	P3–C33–C34	110.9 (5)
C14–C13–C18	104.1 (4)	C33–C34–C35	113.8 (5)
C13–C14–C15	106.1 (4)	C33–C34–C37	123.4 (6)
C14–C15–C16	104.9 (5)	C35–C34–C37	122.9 (6)
C14–C15–P2	100.7 (4)	C34–C35–C36	114.1 (5)
C16–C15–P2	101.5 (4)	C34–C35–C38	120.5 (6)
C15–C16–C17	109.7 (5)	C36–C35–C38	125.5 (7)
C15–C16–C19	121.4 (5)	P3–C36–C35	110.7 (5)
C17–C16–C19	128.7 (6)	C40–C39–C43	108.8 (7)
C16–C12–C18	111.3 (5)	C39–C40–C41	107.0 (6)
C16–C17–C20	128.1 (5)	C40–C41–C42	109.0 (6)
C18–C17–C20	120.6 (5)	C41–C42–C43	107.5 (6)
C13–C18–C17	110.1 (4)	C39–C43–C42	107.6 (6)
C13–C18–P2	95.3 (3)	C27–C32–C31	119.6 (7)

[a] Numbers in parentheses are estimated standard deviations in the least significant figures.

is anticipated to be formed. Two products were observed in a 5:1 ratio when reaction 9 was conducted at 80 °C, but only one was observed in a reaction performed for 48 h at 25 °C. Each of the products is a racemic mixture of two enantiomeric diastereomers. These two diastereomeric pairs were separated by fractional crystallization, and the minor diastereomer (**4b**) was characterized by X-ray crystallography (vide infra).

Reaction 10 yielded two mono Diels–Alder products (**5a,b**) in a 3:1 ratio and a meso bis Diels–Alder product (**5c**) in an amount equal to the sum of **5a** and **5b**; **5c**, the less soluble product, separates from solution as it is formed. **5c** was also characterized by X-ray crystallography (vide infra). Prolonged heating of **5a,b** even in the presence of additional DVPP caused no conversion of either **5a** or **5b** into **5c**. This suggested that (1) the vinyl groups on the exocyclic phosphorus in these two compounds are anti to the coordinated phosphole and (2) no inversion of the configuration of the exocyclic phosphorus occurs under these conditions. Ru–P bond rupture would be required in order for phosphorus inversion to occur. Four mono Diels–Alder products should be possible in the first cycloaddition reaction, leading to four possible bis Diels–Alder products. That only one bis Diels–Alder product is formed illustrates the high diastereoselectivity of this reaction. Reactions 16 and 17 exhibited higher diastereoselectivities than reactions 9 and 10, with the diastereomeric ratios being 9:1 and 6:1, respectively. **6a** was separated from **6b**, but **7a** could not be separated from **7b**. Only one pair of racemic diastereomers was formed in reactions 13–15.

It was previously found[2,4,7,8] that diallylphenylphosphine (DAPP) would not undergo intramolecular [4 + 2] Diels–Alder cycloaddition with coordinated DMPP. We concluded that this was due to the poor dienophilicity of DAPP and not to steric effects. Considering that the ruthenium center in the $[(\eta^5\text{-}C_5H_5)Ru(PR_3)_3]PF_6$ complexes is more electron rich than the metal centers previously studied, we reasoned (1) that it may polarize its coordinated ligands to a greater extent and therefore better

activate them toward cycloadditions and (2) the relative orientation of the coordinated ligands in this piano-stool system may provide better molecular orbital overlap of the diene and dienophile, thus also better promoting [4 + 2] cycloadditions than for the other systems thus far studied. As DAPP is a poor dienophile, the initial product of reaction 11 is the ligand substitution product $[(\eta^5\text{-}C_5H_5)\text{-}Ru(DMPP)_2(DAPP)]PF_6$ (**8**). However, three Diels–Alder products (**9a–c**) were ultimately formed upon heating the reaction mixture for longer time periods (reaction 12).

The $^{31}P\{^1H\}$ NMR spectrum of the bis Diels–Alder product (**9c**) indicated that the tridentate ligand so formed is a *dl* diastereomer rather than a meso diastereomer as was found for **5c** (reaction 10). **9a** was the major product in reaction 12. **9a–c** are each racemic mixtures of two enantiomeric diastereomers. They were separated by column chromatography on silica gel.

The results of reaction 12 indicate that the stereochemistry of the products is influenced by both electronic and steric effects. Molecular models suggest that the major reason that a Diels–Alder cycloaddition did not occur for the other metal systems, with either square-planar or octahedral coordination geometries, is mainly because of the geometry within the coordination sphere and is not a sole result of the poor dienophilicity of DAPP. In these other cases, the carbon–carbon double bond of the allyl group and the diene moiety of DMPP simply cannot be suitably oriented to provide for effective orbital overlap.

The high diastereoselectivity of reactions 13–15 suggests that the diastereoselectivity is controlled not only by steric effects but also by another factor that we will call π-stacking. This π-stacking is evidenced in the crystal structure of **11** (vide infra), wherein the phenyl group attached to the 7-phospha phosphorus atom is stacked on the phosphole ring of the unreacted phosphole. Molecular models suggest that this π-stacking is probably present in **10** and **12** as well.

Complex **11** was observed by variable-temperature $^{31}P\{^1H\}$ NMR spectroscopy (Figure 1) to be dynamic in solution, undergoing rapid sulfur inversion, as is commonly observed for complexes of sulfides.[30] Thus, the $^{31}P\{^1H\}$ NMR spectrum of **11** at 30 °C showed broad singlets for its 7-phospha phosphorus and DMPP resonances. This inversion was stopped at −20 °C, and the equilibrium ratio of the two diastereomers was found to be 3:1 by integration. Thus, one pair of diastereomers is thermodynamically more stable than the other at this temperature by only 2.3 kJ mol^{-1}. The activation energy for sulfur inversion is about[31] 59.8 kJ mol^{-1}, which is near the low end of the typical range for such processes (about 50–71 kJ mol^{-1}).[30b]

The fact that a variety of good dienophiles[32] such as $Me_2NC(O)CH{=}CH_2$, $PhS(O)_2CH{=}CH_2$, and $N{\equiv}C{-}CH{=}CH_2$ did not undergo [4 + 2] Diels–Alder cycloadditions with **1** supports our previous contention[2-8] that all of these reactions are metal-mediated [4 + 2] intramolecular cycloadditions between two coordinated ligands (the diene and the dienophile).

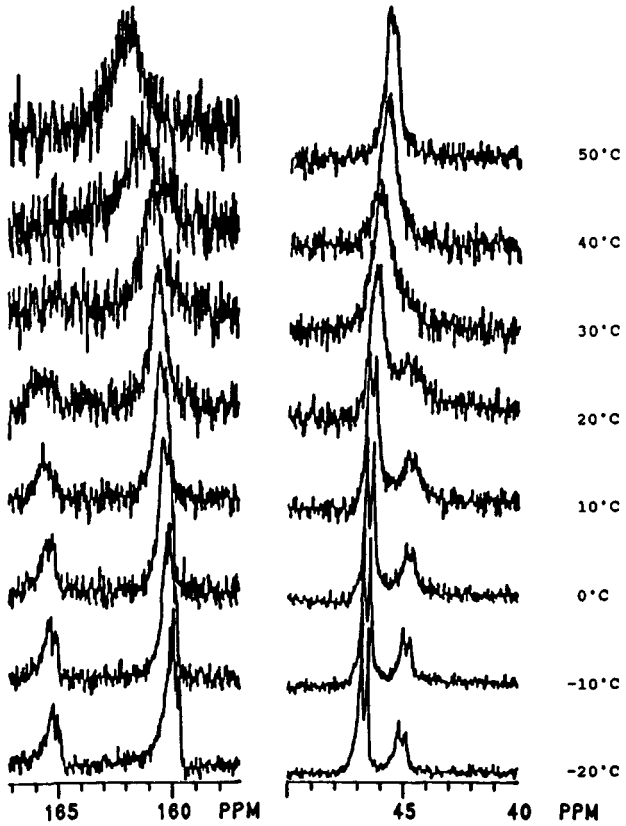

Figure 1. Variable-temperature 121.65-MHz $^{31}P\{^1H\}$ NMR spectra for **11** in $CDCl_3$.

In complexes **14** and **15** there is hindered rotation about the ruthenium–alkene bonds, rendering these two complexes asymmetric. This is evidenced by their AB $^{31}P\{^1H\}$ NMR spectra (Table I). Coordination of the vinyl groups was confirmed by ^1H and $^{13}C\{^1H\}$ NMR spectroscopy (see Experimental Section).

$^{31}P\{^1H\}$ NMR Spectroscopy and Stereochemistry. It was observed (Table I) that the chemical shift difference between the chemical shifts of the two phosphorus nuclei in the chelate ring (P_1 and P_2) is greater for the major diastereomer **4a** ($\Delta\delta$ = 97.02 ppm) than for the minor diastereomer **4b** ($\Delta\delta$ = 82.88 ppm). This observation holds for the $P_1 - P_2$ chemical shift differences of most pairs of diastereomers listed in Table I. Molecular models suggested that **4a** has Ru_RL_S[33] and Ru_SL_R absolute configurations and **4b** has Ru_RL_R and Ru_SL_S absolute configurations. These observations are consistent with an empirical rule,[28] noted by several authors, that for $[(\eta^5\text{-}C_5H_5)Ru(P{\sim}P)L]X$ and $(\eta^5\text{-}C_5H_5)Ru(P{\sim}P)X$ type complexes the diastereomers having the Ru_SL_R configuration exhibit larger ^{31}P chemical shift differences than do those having the Ru_RL_R configuration. This rule should also hold true for the enantiomers Ru_RL_S and Ru_SL_R of these diastereomers such that $\Delta\delta_{^{31}P}(Ru_RL_S) > \Delta\delta_{^{31}P}(Ru_SL_S)$, as enantiomers must have the same chemical shifts in an achiral medium.

Complexes **6a,b**, obtained from the reaction of **2** with DMPP, have $^{31}P\{^1H\}$ NMR spectra very similar to those of **4a,b**, except for the chemical shifts of the unreacted DMPP (**4a,b**) and DPVP (**6a,b**) ligands. It is therefore concluded that **6a**, like **4a**, has the Ru_RL_S and Ru_SL_R

(30) (a) Abel, E. *Chem. Br.* **1990**, 148. (b) Orrell, K. G. *Coord. Chem. Rev.* **1989**, *96*, 1. (c) Zhang, C.; Reddy, H. K.; Schlemper, E. O.; Schrauzer, G. N. *Inorg. Chem.* **1990**, *29*, 4100. (d) Haake, P.; Turley, P. C. *J. Am. Chem. Soc.* **1967**, *89*, 4611. (e) Turley, P. C.; Haake, P. *J. Am. Chem. Soc.* **1967**, *89*, 4617.

(31) Bovey, F. A. *Nuclear Magnetic Resonance Spectroscopy*, 2nd ed.; Academic Press: San Diego, CA, 1988; pp 291 ff.

(32) Carr, R. V. C.; Paquette, L. A. *J. Am. Chem. Soc.* **1980**, *102*, 853. Paquette, L. A.; Kinney, W. A. *Tetrahedron Lett.* **1982**, *23*, 131. Paquette, L. A.; Crouse, G. D. *J. Org. Chem.* **1983**, *48*, 141. Paquette, L. A.; Kinney, W. A. *Tetrahedron Lett.* **1982**, *23*, 5122. Carruthers, W. *Cycloaddition Reactions in Organic Synthesis*; Pergamon: New York, 1990.

(33) Absolute configurations are assigned according to the Baird–Sloan modification of the Cahn–Ingold–Prelog priority rules. See: Stanley, K.; Baird, M. C. *J. Am. Chem. Soc.* **1975**, *97*, 6598. Sloan, T. E. *Top. Stereochem.* **1981**, *12*, 1.

Chart II

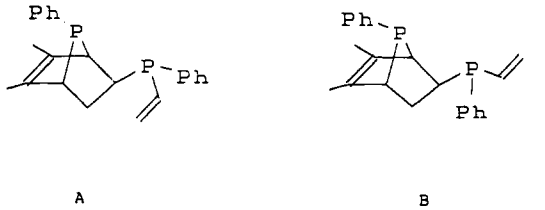

A B

Chart III

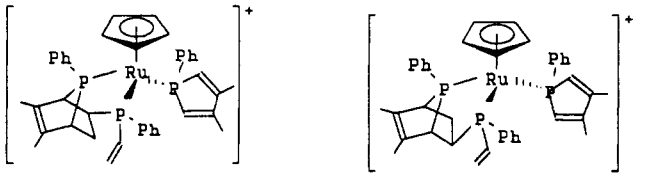

5a 5b

Chart IV

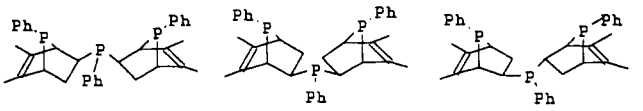

meso-A meso-B d,l

configurations and **6b**, like **4b**, has the Ru_SL_S and Ru_RL_R absolute configurations.

The chemical shift differences between the P_1 and P_2 resonances in **5a** (95.07 ppm) and **5b** (94.52 ppm) are much smaller than the analogous differences observed for **4a,b** or **6a,b**. This indicates that the differences in interligand steric effects between **5a** and **5b** are smaller than for the other complexes. This is also reflected in a smaller ratio of the major to the minor diastereomer (3:1) as compared to 5:1 for **4a**:**4b** and 9:1 for **6a**:**6b**. Since the two substituents on the 2-phosphino phosphorus atom are different in **5a,b**, two diastereomers of the ligands are possible, A and B (Chart II). In similar reactions on Ni,[2] Pd,[3,4] or Pt,[3,4] the A:B diastereomer ratio was greater than 20:1. Molecular models suggest that one of these complexes contains only the A diastereomer of the ligand and the other only the B diastereomer and the structures differ as shown in Chart III.

The $^{31}P\{^1H\}$ NMR spectrum of **5c** showed a first-order AX_2 spin system, with integration showing that the compound contains two 7-phospha phosphorus nuclei. Thus, **5c** is a bis Diels–Alder product arising from a second cycloaddition of one or both of the precursors **5a**′ and **5b**′. The AX_2 pattern in the spectrum indicates that this compound possesses a plane of symmetry which must also be present in the tridentate ligand. This ligand thus has a meso configuration similar to that for the triphosphine that was formed on nickel[2] (reaction 6). The meso configuration was confirmed by ^1H and $^{13}C\{^1H\}$ NMR spectroscopy and X-ray crystallography (vide infra), but careful examination of the X-ray crystal structures shows that the two meso triphosphines are diastereomers of one another, possessing opposite absolute configurations of the central phosphorus atoms. On ruthenium the *meso*-A diastereomer is formed, whereas on nickel the *meso*-B diastereomer (Chart IV) is the product. In neither case were the *dl* diastereomers observed.

Similar to the reaction of 1 with the double dienophile DVPP, its reaction with DAPP also gave three Diels–Alder products: **9a–c**. The $^{31}P\{^1H\}$ chemical shifts of their chelate ring phosphorus nuclei occur somewhat upfield of those in **4–7**. An obvious reason for this is the formation of six-membered chelate rings in **9a,b** in contrast to the

Scheme I

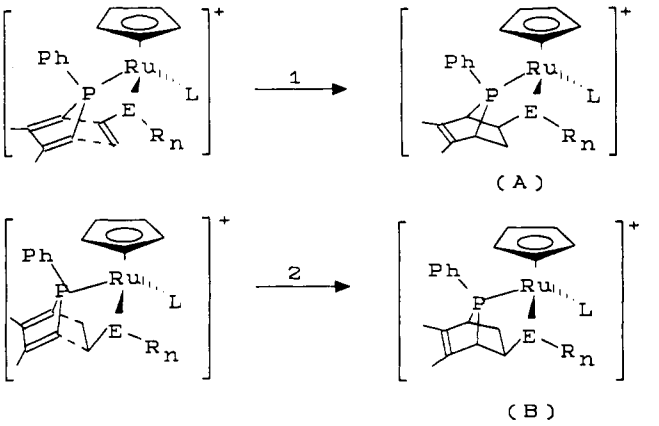

(A) (B)

five-membered rings in the other complexes. Formation of a five-membered ring causes a downfield ^{31}P chemical shift and a six-membered ring an upfield chemical shift, as is typically observed for coordinated diphosphines.[34] The ABX spectrum of **9c** indicates that there is no symmetry element in this complex or in the triphosphine ligand. Thus, this ligand is a *dl* rather than a meso diastereomer. In some instances trace amounts of the meso diastereomer ($\delta_{^{31}P}$ 124.11 (d), 6.51 (t); $^2J(PP)$ = 45.56 Hz) were observed in the crude reaction mixture.

Diastereoselectivity. 1. Syn-Exo Selectivity. All of the [4 + 2] Diels–Alder cycloadditions between the diene (DMPP) and dienophiles (DPVP, DVPP, DAPP, PhSVy, PhS(O)Vy, and 2-vinylpyridine) took place within the coordination sphere of the Ru center. Thus, the activated DMPP and dienophiles undergo intramolecular [4 + 2] cycloadditions, affording only syn-exo (two lone pairs at phosphorus and another donating atom have the syn orientation and the conjugation of E ligands on the norbornene ring has the exo configuration) bidentate chelating ligands with a rigid norbornene backbone (as in Chart I).

2. Regioselectivity. In principle, the two regioisomeric adducts A and B could be formed in these reactions, as either face of the vinyl group on the *E* atom could react (Scheme I). Two regioisomeric adducts have been observed in most reactions, with one predominating, but in some cases only one regioisomeric adduct was formed. The regioselectivity is mainly governed by the steric effects posed in the transition state between the emerging norbornene ligand and the ancillary L ligand. Molecular models demonstrate that the intramolecular steric interactions in the transition state for the formation of regioisomer A are smaller than for the formation of regioisomer B; therefore, regioisomer A should predominate in all these [4 + 2] cycloaddition reactions. This assumption has been proved by single-crystal X-ray structure analysis of three complexes, **4b**, **5c**, and **11**. Because this regioselectivity is mainly affected by steric effects, the bigger the difference in the steric effects between two regioisomers, the higher the regioselectivity. The biggest difference was seen for the two regioisomeric products of reactions **13–15**, where only one regioisomer was formed in each reaction.

It is interesting to note that this regioselectivity does not exist in the square-planar and octahedral systems previously studied when the two R groups are the same. When the two R groups on the E atom are not the same, this regioselectivity may exist but then the steric effects arise in the bidentate ligand itself, either between hydrogens on the norbornene ring and vinyl protons or between

(34) Garrou, P. E. *Chem. Rev.* **1981**, *81*, 229.

Chart V. Four Possible π-Stacking Structures

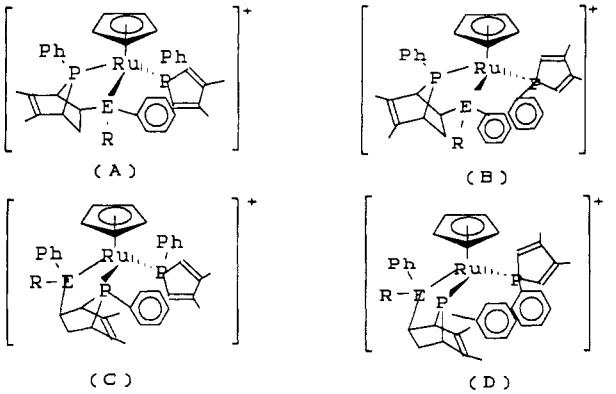

hydrogens on the norbornene ring and phenyl ring protons when R = phenyl and vinyl. For the piano-stool ruthenium system this regioselectivity exists all the time, no matter whether the two R groups are the same or not.

3. π-Stacking Selectivity. The exclusive formation of a single regioisomer in the [4 + 2] cycloaddition reactions of $[(\eta^5\text{-}C_5H_5)Ru(DMPP)_2(CH_3CN)]PF_6$ with the dienophiles phenyl vinyl sulfide, phenyl vinyl sulfoxide, and 2-vinylpyridine suggests that the regioselectivity in these reactions may be facilitated by another factor, "π-stacking". This π-stacking could exist between the phenyl group on the E atom and the phenyl group or phosphole ring of the phosphole ligand (A and B in Chart V). Davies[35] has extensively used this notion in a variety of asymmetric syntheses with the chiral auxiliary $[(\eta^5\text{-}C_5H_5)Fe(CO)PPh_3]$. π-Stacking could also exist between the phenyl group on the bridging phosphorus and the phenyl group or phosphole ring of the phosphole ligand (C and D in Chart V).

The X-ray crystal structure analysis of complex **11** indicates that π-stacking of form C actually exists in the solid state. This π-stacking aided the regioselectivity in this reaction, since other regioisomers do not have this kind of π-stacking. Since for all of the mono [4 + 2] cycloaddition reactions conducted on the $(\eta^5\text{-}C_5H_5)Ru^{II}$ moiety either a phosphole ligand or a ligand containing a phenyl group are present, one may assume that this π-stacking exists in all of the [4 + 2] cycloadducts. The lower regioselectivity observed in some reactions implies that π-stacking is less important and there the steric effects dominate. Analogous regiocontrol by π-stacking has been observed in several purely organic Diels–Alder reactions.[36]

From the above discussion it is concluded that the [4 + 2] cycloaddition reactions between DMPP and dienophile ligands on the piano-stool ruthenium center are kinetically controlled and the diastereoselectivity is greatly influenced by intramolecular steric congestions and π-stacking. Coordination of both the diene (DMPP) and the dienophile to the ruthenium center fixes the *syn-exo*-norbornene configuration. The steric congestion around ruthenium and π-stacking make the conjugation on the inner carbon of the norbornene ring favored over that on the outer one. The diastereoselectivity is greatly affected by a delicate balance among these effects. The best diastereoselectivity is achieved with the dienophiles phenyl vinyl sulfide, phenyl vinyl sulfoxide, and 2-vinylpyridine, leading to only one product. In these three reactions the simultaneous regioselectivity and π-stacking selectivity operate in the same direction. In other reactions the π-stacking may be overcome by steric effects, and more than one racemate is formed.

Scheme II. Structures of Two Racemates from the Reaction of $(\eta^5\text{-}C_5H_5)Ru(Ph_3P)_2Cl$ with P~P

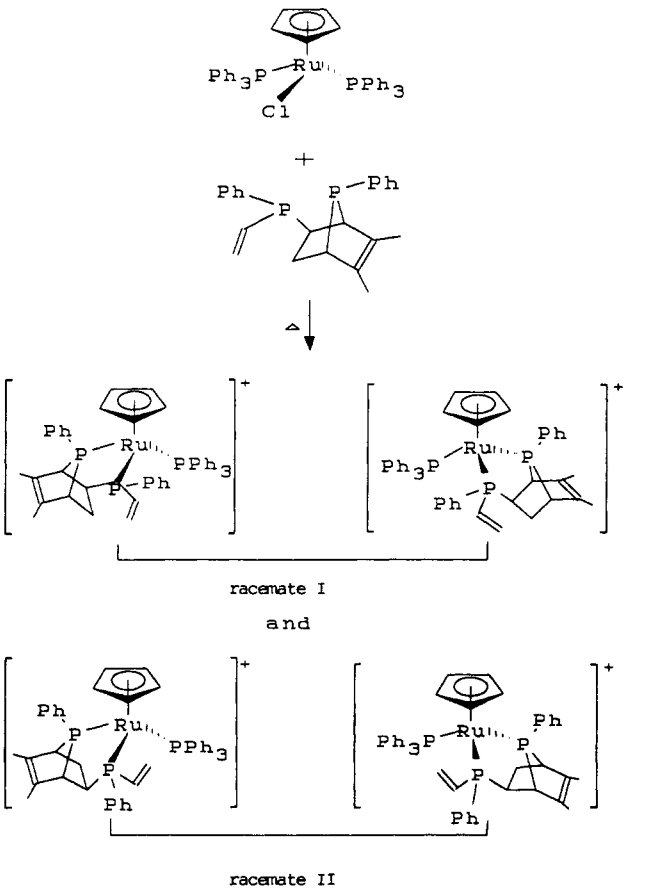

Reactions of $(\eta^5\text{-}C_5H_5)Ru(Ph_3P)_2Cl$. The reaction of $(\eta^5\text{-}C_5H_5)Ru(Ph_3P)_2Cl$ with the bidentate ligand (5,6-dimethyl-7-phenyl-7-phosphabicyclo[2.2.1]-hept-5-ene-2-yl)vinylphenylphosphine, displaced from its $PdCl_2$ complex[3,4] by NaCN in 1,2-dichloroethane afforded the two ionic racemates **13a,b**, which contrasts with the reactions of $(\eta^5\text{-}C_5H_5)Ru(Ph_3P)_2Cl$ with many bidentate biphosphine ligands[28a] in benzene solution, where two neutral diastereomers are obtained. The formation of ionic compounds is probably due to the polar solvent and the presence of the sterically unencumbered 7-phospha phosphorus atom in this ligand. Two racemates were formed in a 3:2 ratio, which is close to the ratio for most reactions of $(\eta^5\text{-}C_5H_5)Ru(Ph_3P)_2Cl$ with biphosphine ligands.

Since the stereocenters in the bidentate ligands are fixed, the two racemates formed should have the geometries shown in Scheme II. They differ in both the configuration of the metal centers and the absolute configuration of the chelate ligand. On the basis of molecular models and comparison of phosphorus NMR data with those of complexes **5** and **7**, the major product was assigned structure I and the minor product was assigned structure II.

Monosubstituted Olefin Complexes. Because there is hindered rotation about the metal–olefin bond in the monosubstituted olefin complexes **14** and **15**, four extreme conformations may be considered (Chart VI). Of these, models clearly indicate that, for conformations III and IV, in which the olefin axis is either in or near the $(\eta^5\text{-}C_5H_5)Ru^{II}(DMPP)_2$ group asymmetry plane, substantial steric interactions exist between C_5H_5 ring protons or the phosphole ligands and the olefin ligand.

(35) Davies, S. G. *Aldrichim. Acta* **1990**, *23*, 31.
(36) Trost, B. M.; O'Krongly, D.; Belletire, J. L. *J. Am. Chem. Soc.* **1980**, *102*, 7595.

Chart VI. Four Possible Conformations of Monosubstituted Olefin Complexes

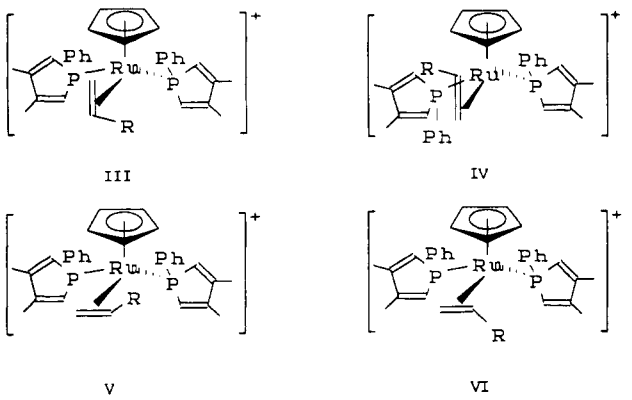

III IV

V VI

A clear distinction cannot be made on steric grounds between V and VI, since interactions exist in each case between the olefin substituent and the η^5-C_5H_5 ring, the phenyl ring, protons, or a phosphole ligand. As a matter of fact, both configurations (V and VI) have been found for similar olefin complexes.[37] However, close examination of the NMR spectral data for these two complexes provides grounds for concluding that the conformation is close to the idealized form VI.

X-ray Crystal Structure Analysis. It appears that the diastereoselectivity and the type of diastereomers formed from the [4 + 2] cycloadditions on the metal mainly depend on steric effects within the coordination sphere. In order to prove our predictions of the diastereoselectivities of thermal intramolecular [4 + 2] cycloadditions in the piano-stool ruthenium system, we have carried out three single-crystal X-ray structure analyses. Each of them represent a different type of complex. They are a bidentate diphosphine complex, a phosphorus–nonphosphorus mixed-ligand complex, and a triphosphine ligand complex. It was discovered that all our predictions from molecular models and NMR data are consistent with the crystallographic results.

1. Molecular Structure of 5c. Since the triphosphine chelating ligand in complex **5c** was synthesized in the piano-stool system, we thought that it may have a structure different from the one formed on nickel and transferred to Ru. It turned out that the two ligands indeed do have different structures. An ORTEP view of one of the cations of **5c** is shown in Figure 2. Final atom coordinates are given in Table III and selected bond lengths and angles in Tables IV and V, respectively. As can be seen from Figure 2, **5c** has a piano-stool geometry defined by the triphosphine and the η^5-cyclopentadienyl ligands. The triphosphine ligand possesses a mirror plane which passes through Ru, the exocyclic phosphorus P2, six carbons of the phenyl ring (C15–C20) on the exocyclic phosphorus, and C21 of the cyclopentadienyl ring and bisects the triphosphine ligand. The halves of the ligand are identical. Though the tridentate ligands formed by reaction between two DMPP ligands and a DVPP ligand on nickel[2] and on ruthenium are both meso, they give rise to different coordination geometries. The ligand L coordinates to Ru in **5c** in a facial fashion and L′ to ruthenium in L′Ru-$(Ph_3P)Cl_2$ in a meridional fashion,[2] and L and L′ are diastereomers of one another. The difference arises from the stereochemistries of the central phosphorus atom, as shown schematically in Chart IV. **5c** contains the *meso*-A diastereomer, while with nickel the *meso*-B diastereomer is

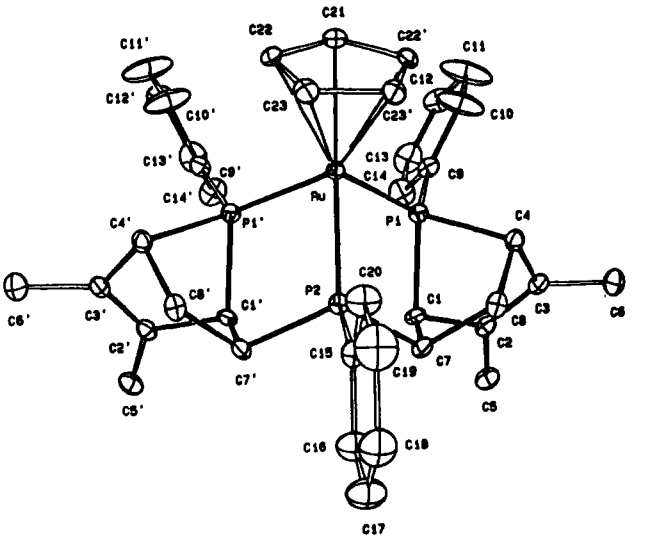

Figure 2. ORTEP drawing of the cation of **5c** showing the atom-numbering (50% probability ellipsoids). Hydrogen atoms are omitted.

the product. The different stereochemistries of L and L′ cause the P1–Ru–P1 angles to be significantly different from each other (97.77 (6)° for **5c** and 157.5 (2)° for L′Ru$(Ph_3P)Cl_2$). It was also found that the Ru–P1 (2.320 (1) Å) and Ru–P3 (2.350 (1) Å) bond distances are longer than the Ru–P2 bond distance (2.308 (1) Å) in L′Ru-$(Ph_3P)Cl_2$, whereas Ru–P1 and Ru–P1′ (2.247 (1) Å) are shorter than Ru–P2 (2.283 (1) Å) in **5c**. All three Ru–P bond distances in **5c** are shorter than those in L′Ru-$(Ph_3P)Cl_2$, implying that the *meso*-A diastereomer, L, is a better donor than the *meso*-B diastereomer, L′.

The C–P–C angles defined by the bridgehead carbons and the 7-phospha phosphorus atoms (80.7 (2)° in **5c**) are slightly larger than those (79.1 (2) and 79.5 (2)°) in L′Ru$(Ph_3P)Cl_2$. These angles are similar to those found in bidentate 7-phosphanorbornene complexes of the Ru-$(CO)Cl_2$(DMPP)(P∼P) type[7] but smaller than those in palladium(II) complexes[3,4] (82.5 (6) and 82.3 (4)°). The three P–Ru–P angles in **5c** (P1–Ru–P2 = P1′–Ru–P2 = 80.00 (4)°, P1–Ru′–P1′ = 96.77 (6)°) are respectively smaller and larger than 90°. The short bond lengths (1.328 (6) Å between C2 and C3, and C2′ and C3′) confirm the presence of double bonds between these atoms. All other angles and bond lengths are normal.

2. Molecular Structure of 11. As previously pointed out, the reactions of **1** with the dienophiles phenyl vinyl sulfoxide and 2-vinylpyridine produced only one diastereomer. The reaction with phenyl vinyl sulfide also gave one racemic diastereomer, but in solution an equilibrium mixture of two interconverting diastereomers was observed. The rapid sulfur inversion does not change the ruthenium, 7-phospha phosphorus, or conjunction carbon in the norbornene ring absolute configurations. The inversion barrier is not large, and this complex crystallized as a single diastereomer, as shown in Figure 3. Final atom coordinates are given in Table VI, and selected bond distances and angles are given in Tables VII and VIII, respectively. The bond angles and distances within the norbornene ring are similar to those of **5c**. The C1–P1–C4 bond angle (79.9 (4)°) is only 0.8° smaller than the corresponding angle for **5c**. The C2–C3 distance (1.33 (1) Å) indicates a double bond. The two Ru–P bond distances are equal (Ru–P1 = 2.280 (2) Å and Ru–P2 = 2.281 (2) Å) and are about the same as those in **5c**. The Ru–S bond distance (2.357 (2) Å) is significantly longer than the Ru–P bond distances. The Ru–S distance is slightly shorter than those reported

(37) Bodner, G. S.; Peng, T. S.; Arif, A. M.; Gladysz, J. A. *Organometallics* **1990**, *9*, 1191 and references therein.

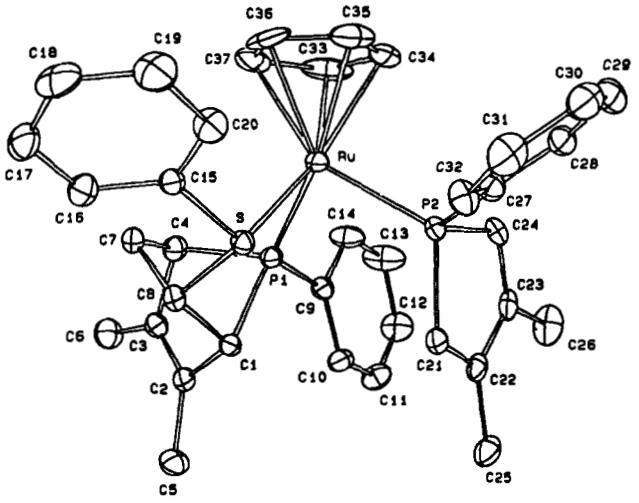

Figure 3. ORTEP drawing of the cation of **11** showing the atom-numbering scheme (50% probability ellipsoids). Hydrogen atoms are omitted.

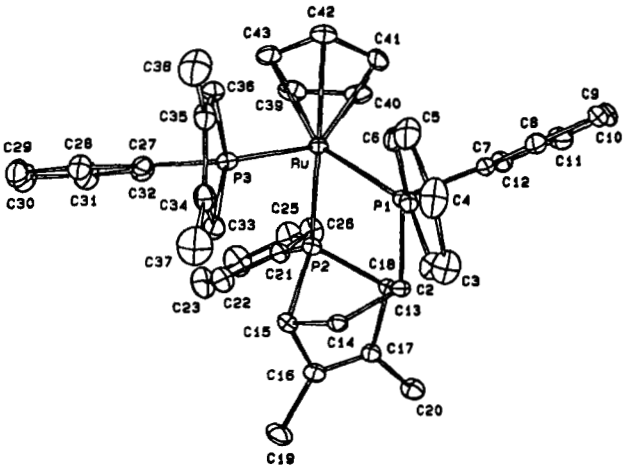

Figure 4. ORTEP drawing of the cation of **4b** showing the atom-numbering scheme (50% probability ellipsoids). Hydrogen atoms are omitted.

for $[(\eta^5\text{-}C_5H_5)Ru(dppm)(Bu^tSH)]PF_6$[38] (2.371 (2) Å) and $[(\eta^5\text{-}C_5H_5)Ru(PPh_3)_2(Pr^nSH)]BF_4$[39] (2.377 (2) Å), probably because the sulfur donor is contained in a five-membered chelate ring in **11**. That the Ru–P bond is shorter than the Ru–S bond in **11** indicates that sulfur is more weakly bound to ruthenium than is phosphorus, as the sulfur radius (1.03 Å) is smaller than the phosphorus radius (1.10 Å).[40] The C1–P1–C9 (108.8 (4)°) and C4–P1–C9 (108.4 (4)°) angles show that the phenyl ring is tilted slightly away from the norbornene ring, as is the case for all analogous [4 + 2] cycloaddition products of DMPP. The plane of this phenyl ring is parallel to the plane of the phosphole ring, providing good π-orbital overlap.

As anticipated, **11** is the regioisomer having the conjunction at the inner carbon of the norbornene ring. The phenyl group on sulfur has a syn orientation relative to the norbornene ring system, avoiding large steric interactions. We believe that the major diastereomer in solution has this same structure, as it has the minimum interligand steric interactions. Compounds **10** and **12** should have similar structures.

3. Molecular Structure of 4b. The reaction of **1** with DPVP produced two racemic diastereomers in a 5:1 ratio. The structure of **4b** (the minor diastereomer) is shown in Figure 4. Final atom coordinates are given in Table IX, and selected bond distances and angles are given in Tables X and XI, respectively. Complex **4b** indeed has the conformation with the outer carbon conjugation to the norbornene ring as expected. As can be seen from the data in Tables X and XI, the angles around ruthenium, the Ru–P bond distances and angles, and bond distances within the norbornene ring are very similar to those of **5c** and **11**. The Ru–P2 bond distance (2.274 (2) Å) is very close to the Ru–P2 bond distance (2.280 (2) Å) in **11**, but the Ru–P1 (2.310 (1) Å) and Ru–P3 (2.317 (2) Å) distances are slightly longer. The C15–P2–C18 angle (80.9 (3)°) is also very close to the corresponding angles in **5c** (80.7 (2)°) and **11** (79.9 (4)°). The rest of the bond angles and distances are normal.

It can be seen from Figure 4 that there is a large steric interaction between the phosphole ligand (DMPP) and the phenyl ring on the 7-phospha phosphorus. This is the main reason this is the less favored diastereomer. The major diastereomer should have an inner carbon conjunction to the norbornene ring, as found for **5c**. For the inner conjunction diastereomer, the 7-phospha phosphorus phenyl group is moved away from the phosphole ligand, avoiding steric interactions between the phenyl ring and the phosphole ligand. Furthermore, **4b** may then possess the π-stacking shown for **11** in Figure 3.

Reaction Mechanism and Reactivity of Dienophiles. All of the bidentate or tridentate ligands with the norbornene backbone have exclusively the syn-exo structure, which implies that the [4 + 2] cycloaddition reactions take place within the metal coordination sphere. DMPP and dienophiles do not undergo [4 + 2] cycloaddition reactions in the absence of a metal, even when heated in a sealed ampule under nitrogen for months. Furthermore, when poor dienophiles such as DAPP were used, the substitution products were first isolated. Therefore, the first step of the reaction involves substitution of the last acetonitrile by a dienophile (eq 18).

$$[(\eta^5\text{-}C_5H_5)Ru(DMPP)_2(CH_3CN)]PF_6 + \text{dienophile} \rightarrow [(\eta^5\text{-}C_5H_5)Ru(DMPP)(\text{dienophile})]PF_6 + CH_3CN \quad (18)$$

In the second step, the coordinated diene and dienophile are electronically activated by the metal and undergo an intramolecular [4 + 2] Diels–Alder cycloaddition reaction in a syn fashion (eq 19), affording a complex containing

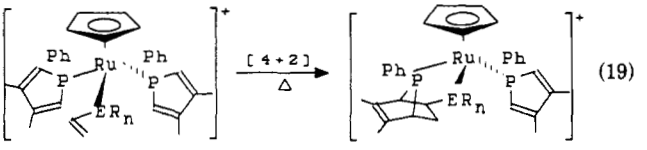

(19)

a chiral bidentate ligand. It is this step that determines the diastereoselectivity of the reaction, which is affected by the simultaneous operation of several factors: metal template, intramolecular steric effects, and the π-stacking model. With the double dienophiles DVPP and DAPP, two consecutive [4 + 2] cycloadditions occurred to afford complexes containing tridentate ligands (eq 20). The diastereoselectivity in this step is dictated by asymmetric induction from the mono Diels–Alder product in addition to the above-mentioned factors.

Although all six dienophiles DPVP, DVPP, DAPP, PhSVy, PhS(O)Vy, and 2-vinylpyridine underwent [4 + 2] cycloadditions with the $(DMPP)_2(\eta^5\text{-}C_5H_5)Ru^{II}$ moiety,

(38) Conroy-Lewis, F. M.; Simpson, S. J. *J. Chem. Soc., Chem. Commun.* **1991**, 388.
(39) Amarasekera, J.; Rauchfuss, T. B. *Inorg. Chem.* **1989**, *28*, 3875.
(40) Huheey, J. E. *Inorganic Chemistry*, 3rd ed.; Harper and Row: New York, 1983; p 258.

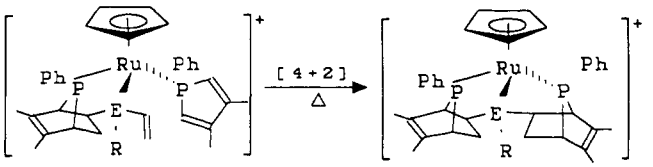

(20)

they do not do so with equal ease. DAPP is the least reactive, and 2-vinylpyridine is the most reactive. Since two sequential steps were involved in the mono [4 + 2] cycloadditions, the overall rates were determined by the rates in these two steps. Which one is the rate-determining step?

There are two possible mechanisms (dissociative or associative) for the substitution step. For the five dienophiles $Ph_2PCH{=}CH_2$, $PhP(CH{=}CH_2)_2$, $PhSCH{=}CH_2$, $PhS(O)CH{=}CH_2$, and 2-vinylpyridine, the substitution products could not be observed, which indicates that the intramolecular [4 + 2] cycloadditions are virtually instantaneous for them. Thus, the rate-determining step is the first step. If the ligand substitution in the first step involves a dissociative mechanism, the dienophile reactivities should be about the same. This is because the nature of the entering group has very little influence on the rate of dissociative reactions.[41] However, their reaction rates are very different. This suggests that the substitution step may involve a dissociative interchange (I_d) mechanism. The better and smaller the nucleophile, the faster the reaction. Therefore, the reactivity of the five dienophiles should be in the order 2-Vypy > PhSVy > PhS(O)Vy > $PhPVy_2$ > Ph_2PVy, which is in agreement with the experimental observations. This mechanism is consistent with the observations of Ludi and co-workers,[26] who found that ligand substitutions of $[(\eta^5\text{-}C_5H_5)Ru(CH_3CN)_3]^+$ proceed by dissociative or dissociative-interchange pathways. For the dienophile DAPP, the substitution product was observed and isolated. This suggests that the intramolecular cycloaddition is relatively slow for it and is now the rate-determining step. This also suggests that the reactivity observed for the above five dienophiles is a function of their relative dienophilicities. The dienophilicity of dienophiles is enhanced by an adjacent electron-withdrawing group; thus, the dienophilicity of the six dienophiles might be in the order 2-Vypy > PhS(O)Vy ≈ PhSVy > Ph_2PVy ≈ $PhP(Vy)_2$ > $PhP(allyl)_2$, which is also consistent with the relative experimentally observed cycloaddition rates.

Redox Properties of the Complexes. The electron-donor abilities of coordinated ligands and the complex geometry greatly affect the redox potentials of ruthenium complexes.[42,43] The electrochemical behavior of several of the complexes prepared in this study was investigated by cyclic voltammetry (Table XII). For all complexes the Ru(II)/Ru(III) redox couple is a quasi-reversible one-electron process or a process that approaches reversibility. For **1**, **5c**, **11**, and **12**, the follow-up chemical step is slow and reversible voltammograms were observed. For **15**, both a quasi-reversible one-electron oxidation and reduction were observed. For the other complexes, the follow-up chemical step is fast, as no cathodic wave could be seen on the return sweep, even at high scan rates. In the case of **15**, E_{max} was determined by differential pulse voltammetry. The peak oxidation potential could not be determined by cyclic voltammetry, since it is too near the limit of the electrode/solvent/supporting electrolyte system used. The data in Table XII are very similar to those reported[21] for $RuCl_2(Ph_nPMe_{3-n})_3(CO)$ and $RuCl_2(Ph_nPMe_{3-n})_2(CO)_2$. The Ru(II)/Ru(III) potentials ranged from 0.52 to 1.24 V for the carbonyl complexes. The $E_{1/2}$ values depend principally upon the σ-donor and/or π-acceptor abilities of the ligands. Comparison of the $E_{1/2}$ values for the oxidations of **1–3** indicates that the σ-donor ability of the three phosphines decreases in the order DMPP > DVPP > DPVP. The σ-donor abilities of ligands are generally in the ordr N > S > P, as shown from the $E_{1/2}$ values of **4a,b**, **5c**, **6a**, **9c**, **11**, and **12**. It was also found that bidentate ligands do not necessarily have better donating abilities than two comparable monodentate ligands, as measured by $E_{1/2}$ values (compare **1–3**, **14**, and **15** with the other complexes).

Table XII. Redox Characteristics of the Complexes[a]

compd no.	complex formula	Ru(II)/Ru(III) $E_{1/2}$, V (ΔE, mV)
1	$[CpRu(DMPP)_2(MeCN)]PF_6$	0.58 (110)
2	$[CpRu(DPVP)_2(MeCN)]PF_6$	0.76[b]
3	$[CpRu(DVPP)_2(MeCN)]PF_6$	0.70[b]
4a	$[CpRu(DMPP)_2(DPVP)]PF_6$ ([4 + 2] A)	0.78[b]
4b	$[CpRu(DMPP)_2(DPVP)]PF_6$ ([4 + 2] B)	0.83[b]
5c	$[CpRu(DMPP)_2(DVPP)]PF_6$ (bis [4 + 2])	0.70 (80)
6a	$[CpRu(DMPP)(DPVP)_2]PF_6$ ([4 + 2])	0.79[b]
9c	$[CpRu(DMPP)_2DAPP]PF_6$ (bis [4 + 2])	0.86[b]
10	$[CpRu(DMPP)_2(PhS(O)Vy)]PF_6$ ([4 + 2])[c]	0.96[b]
11	$[CpRu(DMPP_2(PhSVy)]PF_6$ ([4 + 2])	0.63 (95)
12	$[CpRu(DMPP)_2(2\text{-}VyPy)]PF_6$ ([4 + 2])	0.52 (53)
14	$[CpRu(DMPP)_2(Me_2NC(O)Vy)]PF_6$	0.81[b]
15	$[CpRu(DMPP)_2(PhS(O)_2Vy)]PF_6$	1.23[d]

[a] In CH_2Cl_2 containing 0.1 M TBAP at 25 °C, v = 200 mV s^{-1}. E values are vs Fc^+/Fc. Cp = $\eta^5\text{-}C_5H_5$. [b] E_{pa} only. [c] Ru(II)/Ru(I), −1.96 V, E_{pc} only. [d] E_{max} determined by differential pulse voltammetry (peak oxidation potential could not be determined by cyclic voltammetry since it is too near the limit of the electrode/solvent/supporting electrolyte system used).

Acknowledgment. We are grateful to the donors of the Petroleum Research Fund, administered by the American Chemical Society, for financial support and to Johnson Matthey Aesar/Alfa for their generous loan of ruthenium.

Supplementary Material Available: For the three structures, listings of crystal and refinement data, bond distances and angles, H atom coordinates, and thermal parameters (U) (27 pages). Ordering information is given on any current masthead page.

OM9106802

(41) Basolo, F.; Pearson, R. G. *Mechanisms of Inorganic Reactions*, 2nd ed.; Wiley: New York, 1967.
(42) Lever, A. B. P. *Inorg. Chem.* **1980**, *29*, 1271.
(43) Duff, C. M.; Heath, G. A. *Inorg. Chem.* **1991**, *30*, 2528.